Geosynthetic Reinforced Soil Integrated Bridge System Synthesis Report

PUBLICATION NO. FHWA-HRT-11-027

JANUARY 2011

U.S. Department of Transportation
Federal Highway Administration

Research, Development, and Technology
Turner-Fairbank Highway Research Center
6300 Georgetown Pike
McLean, VA 22101-2296

FOREWORD

Geosynthetic Reinforced Soil (GRS) technology consists of closely-spaced layers of geosynthetic reinforcement and compacted granular fill material. GRS has been used for a variety of earthwork applications since the U.S. Forest Service first used it to build walls for roads in steep mountain terrain in the 1970s. Since then, the technology has evolved into the GRS Integrated Bridge System (IBS), a fast, cost-effective method of bridge support that blends the roadway into the superstructure. GRS-IBS includes a reinforced soil foundation, a GRS abutment, and a GRS integrated approach. The application of IBS has several advantages. The system is easy to design and economically construct. It can be built in variable weather conditions with readily available labor, materials, and equipment and can easily be modified in the field. This method has significant value when employed for small, single span structures meeting the criteria described in this report.

As a result of the demonstrated performance of GRS-IBS, the technology was selected for the Federal Highway Administration's (FHWA) Every Day Counts initiative, aimed at accelerating implementation of proven, market-ready technologies. This report is the second in a two-part series and provides the background and other supporting information to substantiate the design method of GRS-IBS. The first document is a manual covering the design and construction of GRS-IBS. This two-part document series designs GRS as a composite material with known and predictable performance and deformations. Both documents are a collaboration between many disciplines within FHWA: geotechnical, structural, hydraulic, maintenance, and pavement engineering.

Jorge Pagán-Ortiz
Director, Office of Infrastructure
Research and Development

TECHNICAL REPORT DOCUMENTATION PAGE

1. Report No. FHWA-HRT-11-027	2. Government Accession No.	3. Recipient's Catalog No.	
4. Title and Subtitle Geosynthetic Reinforced Soil Integrated Bridge System, Synthesis Report		5. Report Date January 2011	
		6. Performing Organization Code:	
7. Author(s) Michael Adams, Jennifer Nicks, Tom Stabile, Jonathan Wu, Warren Schlatter, and Joseph Hartmann		8. Performing Organization Report No.	
9. Performing Organization Name and Address Office of Infrastructure Research and Development Federal Highway Administration 6300 Georgetown Pike McLean, VA 22181		10. Work Unit No.	
		11. Contract or Grant No.	
12. Sponsoring Agency Name and Address Federal Highway Administration U.S. Department of Transportation Washington, DC		13. Type of Report and Period Covered	
		14. Sponsoring Agency Code	
15. Supplementary Notes The FHWA Contracting Officer's Technical Representative (COTR) was Mike Adams, HRDS-40.			
16. Abstract This report is the second in a two-part series to provide engineers with the necessary background knowledge of Geosynthetic Reinforced Soil (GRS) technology and its fundamental characteristics as an alternative to other construction methods. It supplements the interim implementation manual (FHWA-HRT-11-026), which outlines the design and construction of the GRS Integrated Bridge System (IBS). The research behind the proposed design method is presented along with case histories to show the performance of in-service GRS-IBS and GRS walls.			
17. Key Words Geosynthetic Reinforced Soil (GRS), Integrated Bridge System (IBS), Design, Construction, Performance test, Geosynthetic, Material specifications, Quality assurance, Quality control		18. Distribution Statement	
19. Security Classif. (of this report) Unclassified	20. Security Classif. (of this page) Unclassified	21. No. of Pages 64	22. Price

Form DOT F 1700.7 (8-72) Reproduction of completed page authorized

SI* (MODERN METRIC) CONVERSION FACTORS

APPROXIMATE CONVERSIONS TO SI UNITS

Symbol	When You Know	Multiply By	To Find	Symbol
		LENGTH		
in	inches	25.4	millimeters	mm
ft	feet	0.305	meters	m
yd	yards	0.914	meters	m
mi	miles	1.61	kilometers	km
		AREA		
in^2	square inches	645.2	square millimeters	mm^2
ft^2	square feet	0.093	square meters	m^2
yd^2	square yard	0.836	square meters	m^2
ac	acres	0.405	hectares	ha
mi^2	square miles	2.59	square kilometers	km^2
		VOLUME		
fl oz	fluid ounces	29.57	milliliters	mL
gal	gallons	3.785	liters	L
ft^3	cubic feet	0.028	cubic meters	m^3
yd^3	cubic yards	0.765	cubic meters	m^3
		NOTE: volumes greater than 1000 L shall be shown in m^3		
		MASS		
oz	ounces	28.35	grams	g
lb	pounds	0.454	kilograms	kg
T	short tons (2000 lb)	0.907	megagrams (or "metric ton")	Mg (or "t")
		TEMPERATURE (exact degrees)		
^oF	Fahrenheit	5 (F-32)/9 or (F-32)/1.8	Celsius	^oC
		ILLUMINATION		
fc	foot-candles	10.76	lux	lx
fl	foot-Lamberts	3.426	$candela/m^2$	cd/m^2
		FORCE and PRESSURE or STRESS		
lbf	poundforce	4.45	newtons	N
lbf/in^2	poundforce per square inch	6.89	kilopascals	kPa

APPROXIMATE CONVERSIONS FROM SI UNITS

Symbol	When You Know	Multiply By	To Find	Symbol
		LENGTH		
mm	millimeters	0.039	inches	in
m	meters	3.28	feet	ft
m	meters	1.09	yards	yd
km	kilometers	0.621	miles	mi
		AREA		
mm^2	square millimeters	0.0016	square inches	in^2
m^2	square meters	10.764	square feet	ft^2
m^2	square meters	1.195	square yards	yd^2
ha	hectares	2.47	acres	ac
km^2	square kilometers	0.386	square miles	mi^2
		VOLUME		
mL	milliliters	0.034	fluid ounces	fl oz
L	liters	0.264	gallons	gal
m^3	cubic meters	35.314	cubic feet	ft^3
m^3	cubic meters	1.307	cubic yards	yd^3
		MASS		
g	grams	0.035	ounces	oz
kg	kilograms	2.202	pounds	lb
Mg (or "t")	megagrams (or "metric ton")	1.103	short tons (2000 lb)	T
		TEMPERATURE (exact degrees)		
^oC	Celsius	1.8C+32	Fahrenheit	^oF
		ILLUMINATION		
lx	lux	0.0929	foot-candles	fc
cd/m^2	$candela/m^2$	0.2919	foot-Lamberts	fl
		FORCE and PRESSURE or STRESS		
N	newtons	0.225	poundforce	lbf
kPa	kilopascals	0.145	poundforce per square inch	lbf/in^2

*SI is the symbol for the International System of Units. Appropriate rounding should be made to comply with Section 4 of ASTM E380.
(Revised March 2003)

TABLE OF CONTENTS

LIST OF FIGURES

LIST OF TABLES

CHAPTER 1. GEOSYNTHETIC REINFORCED SOIL INTEGRATED BRIDGE SYSTEM

1.1 INTRODUCTION

The Geosynthetic Reinforced Soil (GRS) Integrated Bridge System (IBS) provides an economical solution to accelerated bridge construction. Employing this technology will help agencies save both time and money in planning and executing projects. This synthesis report and its companion document were developed to assist deployment of this promising technology as part of the Federal Highway Administration's (FHWA) Every Day Counts initiative.[1] This synthesis report provides the background and research behind the recommended design of GRS-IBS outlined in the interim implementation manual.[1] In-service performance of GRS-IBS and other GRS applications is also discussed through case histories.

GRS-IBS is a fast, cost-effective method of bridge support that blends the roadway into the superstructure to create a jointless interface between the bridge and the approach (see figure 1). It consists of three main components: the reinforced soil foundation (RSF), the abutment, and the integrated approach. The RSF is composed of granular fill material that is compacted and encapsulated with a geotextile fabric. It provides embedment and increases the bearing width and capacity of the GRS abutment. It also prevents water from infiltrating underneath and into the GRS mass from a river or stream crossing. This method of using geosynthetic fabrics to reinforce foundations is a proven alternative to deep foundations on loose granular soils, soft fine-grained soils, and soft organic soils.[2] The abutment uses alternating layers of compacted fill and closely spaced geosynthetic reinforcement to provide support for the bridge, which is placed directly on the GRS abutment without a joint and without cast-in-place (CIP) concrete. GRS is also used to construct the integrated approach to transition to the superstructure. This bridge system therefore alleviates the "bump at the bridge" problem caused by differential settlement between bridge abutments and approach roadways.

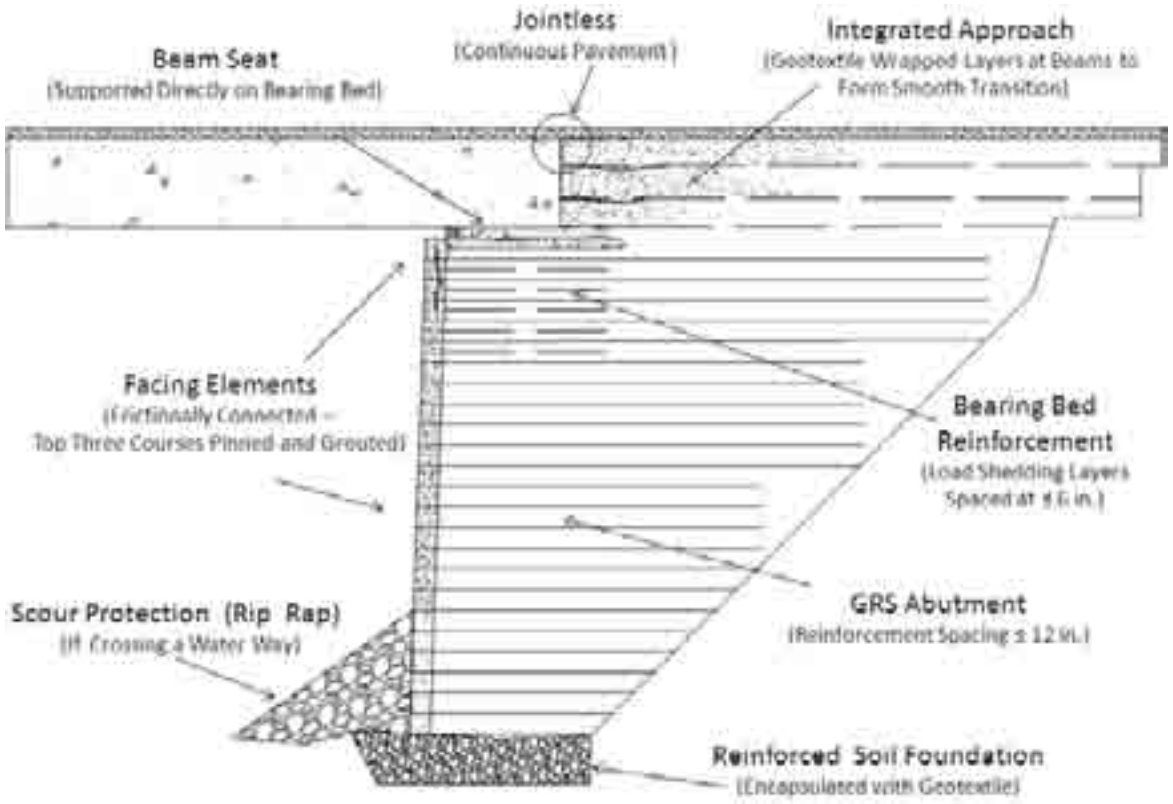

Figure 1. Illustration. Typical GRS-IBS cross section.

1.2 BACKGROUND

Mark Twain said, "The ancients have stolen all our best ideas." Reinforced soil technology is not modern. The ancients used native material such as straw, tree branches, and plant material to reinforce the earth. The reinforcement provides tensile resistance to soil that is weak in tension but relatively strong in compression and shear. Through soil reinforcement interface bonding, the reinforcement restrains lateral deformation of the surrounding soil, increases its confinement, reduces its tendency for dilation, and consequently, increases the stiffness and strength of the soil mass.

In ancient Babylonia, the technology was used to construct the Aqar Quf ziggurat in Iraq around 1440 B.C. The stepped pyramid was built using compacted layers of plant material and soil blocks. The Great Wall of China also used reinforced earth to construct some sections. The fact that these structures are still visible today is a tribute to the durability of reinforced soil technology.

Modern reinforced soil technology has evolved into two primary methods for the stabilization of earth: mechanically stabilized earth (MSE) and GRS. Today, the predominant method of building reinforced soil is MSE, established in the early 1960s when Henri Vidal patented Reinforced Earth®. The method incorporates discrete steel strips embedded within a soil mass. Since then, other types of reinforcement materials, classified as either inextensible or extensible, have been used to reinforce earth. Berg et al. defined *inextensible reinforcement* as a material that deforms considerably less than the surrounding soil at failure and *extensible reinforcement* as a material that deforms as much as the surrounding soil.[3] In fact, MSE technology has branched off into two primary

pathways: proprietary structures built with metallic (inextensible) reinforcements and proprietary structures built with geosynthetic (extensible) reinforcements.

MSE structures built with inextensible reinforcement such as discrete metallic strips or welded wire mats have a unique combination of precast panels, reinforcement, and connection details. The vertical spacing of the reinforcement (S_v) is typically about 30 inches, and the typical size of the precast panels is about 5 ft high by 5 to 10 ft wide (see figure 2 and figure 3).

Figure 2. Photo. MSE inextensible reinforcement—steel strips.[(3)]

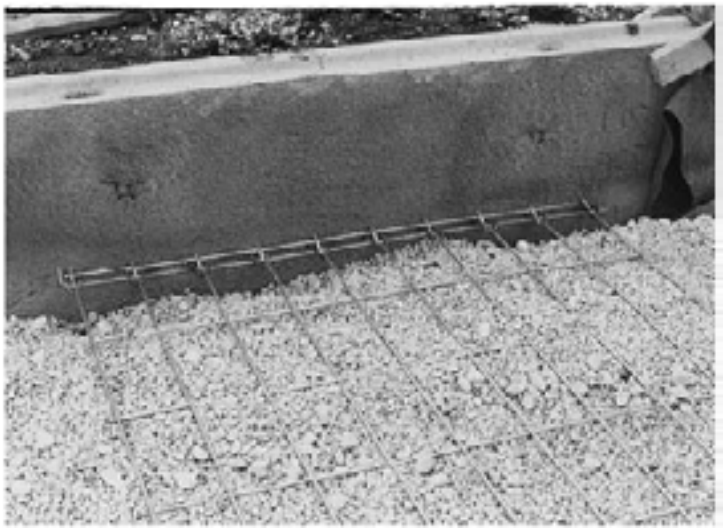

Figure 3. Photo. MSE inextensible reinforcement—wire mats.[(3)]

MSE structures built with extensible reinforcement such as geosynthetics were introduced in the mid-1980s when geogrids were used to reinforce or stabilize the fill behind structures constructed with concrete modular blocks (see figure 4). Today, these proprietary modular block structures are typically built with a unique combination of the block, geogrids, and connection details. The vertical spacing of the reinforcement (S_v) is typically 24 inches, or one layer of reinforcement for every three courses of 8-inch modular block facing. The facing block has typical dimensions of 8 inches by 16 inches by 12 inches and a weight of about 80 lb.

Figure 4. Photo. MSE extensible reinforcement (geogrid).

The first documented use of alternating layers of geosynthetic and soil, referred to as GRS technology, was by the U.S. Forest Service in the 1970s.[4] The Forest Service used the technology to build logging roads on steep mountain terrain. These GRS structures utilized a wrapped face—the geosynthetic was wrapped up and around the face of the individual soil layers and anchored by the overburden of the subsequent layer of soil (see figure 5). Many of these wrapped-face GRS structures (also called burrito walls) are still in service.

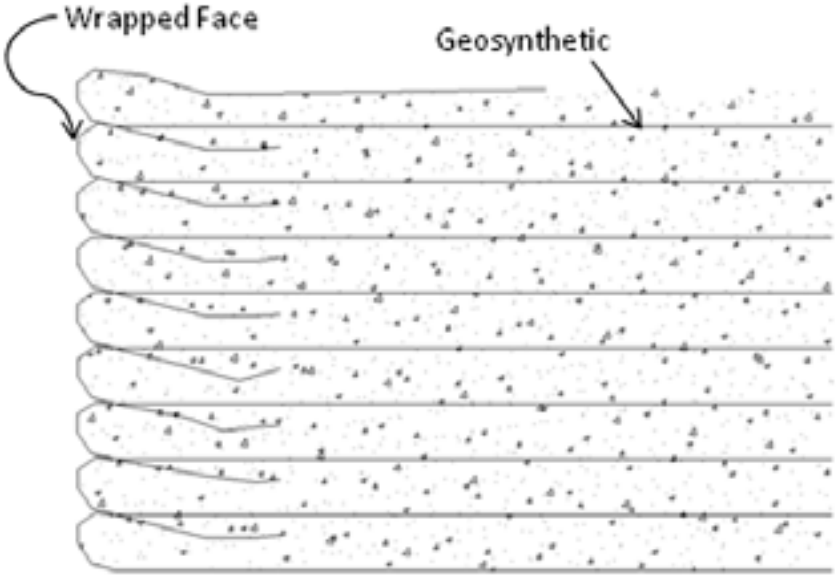

Figure 5. Illustration. Typical wrapped-face GRS structure.

Later, the Colorado Department of Transportation (CDOT) developed a low-cost generic wall system using lightweight concrete modular blocks. Rather than securing the blocks to the reinforcement with connections, as in MSE technology, the concrete facing blocks were frictionally connected to the GRS mass (see figure 6). The interface between the blocks and the geosynthetic provided enough friction to resist block movement. This method of connection in combination with closely

spaced reinforcement layers created a facing system that adjusts to relieve stress without attracting loads. The FHWA refined the CDOT method to account for vertical load-bearing applications, resulting in the development of GRS abutments, followed by GRS-IBS (see figure 1).[5,6]

Figure 6. Photo. Cut-away of GRS mass.

GRS-IBS was initially developed by FHWA during the Bridge of the Future initiative to help meet the demand for the next generation of small, single span bridges in the United States. GRS-IBS can be built with lower cost, faster construction, and potential improved durability and can be used to build bridges on all types of roads, on or off the National Highway System.

As of 2010, 45 bridges utilizing GRS abutments had been built in the United States. Of these bridges, IBS had been employed on 28 bridges, all built over water crossings. The hydraulic environments at these locations is such that scour is shallow, making the system feasible for these sites. Refer to the interim implementation manual for special hydraulic design requirements before selecting a water crossing for GRS-IBS deployment.[1]

1.3 COMPOSITE BEHAVIOR

GRS abutments built with a reinforcement spacing less than or equal to 12 inches behave as a composite mass with predictable behavior. They can be built to economically support a bridge superstructure bearing directly on the reinforced soil behind the facing block. GRS can be used to integrate the superstructure with the approach and substructure to create a jointless bridge system (GRS-IBS).

Many studies have been conducted on the composite behavior of GRS structures. These investigations have concluded that existing design methods do not adequately characterize the interactive behavior between the soil and the closely spaced reinforcement of a GRS

abutment.[3,7] As a result, the interim implementation manual was developed.[1] The manual is largely based on the observed composite behavior of GRS and is substantiated by empirical evidence of in-service GRS-IBS.

1.3.1 Reinforcement Spacing

A degree of composite behavior results from reinforcement frequency. For larger-spaced reinforced soil systems, the composite behavior diminishes with increased reinforcement spacing. It is important to note that the transition into GRS behavior is not dependent solely on reinforcement spacing; the aggregate size and friction angle are also contributing factors, as explained in chapter 3.

Closer reinforcement spacing creates more soil-geosynthetic interaction. In GRS, the reinforcement not only serves to resist tensile forces but also functions to restrain lateral deformation of the soil, increase lateral confinement of the soil, generate apparent cohesion in a granular fill (while maintaining all desirable characteristics of granular soil), suppress dilation of the soil, enhance compaction-induced stresses, increase ductility of the soil mass, and reduce migration of fines, depending on the reinforcement type selected. These added benefits develop because of the close reinforcement spacing.

The frequency of reinforcement spacing in GRS allows for compaction of the soil directly behind the facing, producing the capacity for load bearing at this location. The spacing of the reinforcement also has a significant impact on the strength and behavior of GRS performance. This is illustrated in figure 7, which shows the load-carrying capacity of GRS with a typical spacing of 8 inches.[8] The figure shows that working loads for bridges are about 4 ksf.[9] The ultimate capacity of GRS, however, can be as high as 25 ksf. The ultimate capacity of GRS is a function of the reinforcement spacing, the reinforcement strength, and the soil conditions, including maximum particle size and friction angle.

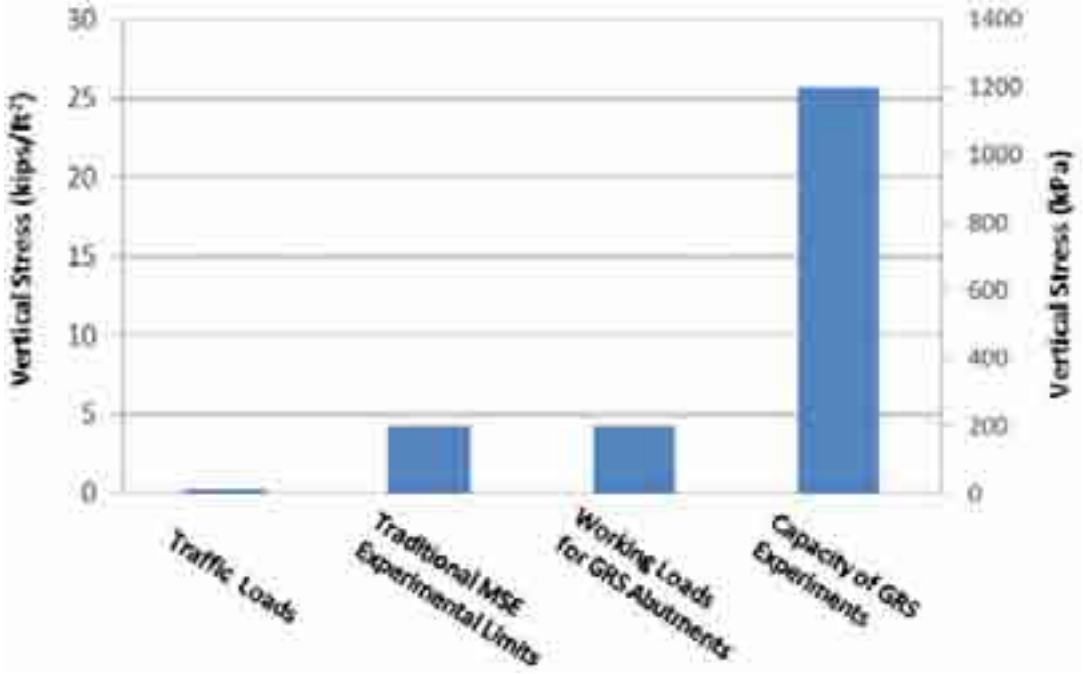

Figure 7. Graph. General comparison of surcharges on MSE and GRS structures.

The ultimate capacity of GRS is influenced more by the reinforcement spacing than by the reinforcement strength (T_f).[10] This is apparent in the results from large-scale tests, shown in table 1. The results indicate that the response is not the same at the same T_f/S_v ratio. The strength of the GRS mass is 1.5 times higher and the stiffness 1.3 times higher at lower spacing and reinforcement strength (test 2) than at higher spacing and reinforcement strength (test 3). Reduced spacing at equal reinforcement strengths (tests 2 and 4) increases the strength of the GRS mass by 2.1 times and the stiffness by 1.3 times. Increasing the reinforcement strength at equal spacing, however, only increases the strength of the GRS mass by 1.4 times and the stiffness by 1.0 times (tests 3 and 4). This shows that spacing has a larger effect than reinforcement strength.

Table 1. Large-scale GRS tests.[10]

	Reinforcement			Confining Stress	Ultimate Applied Vertical Load	Modulus at 1 Percent Vertical Strain	Strain at Failure
	Spacing	Strength	Ratio				
Test	S_v (inches)	T_f (lb/ft)	T_f/S_v	σ_c (ksf)	q_{ult} (ksf)	E @ ε_v = 1% (ksf)	ε_v (Percent)
1	–	4,800	–	0.7	16	700	3
2	8	4,800	600	0.7	56	1,300	6.5
3	16	9,600	600	0.7	36.5	1,000	6.1
4	16	4,800	300	0.7	27	970	4
5	8	4,800	600	0.0	40	1,100	6

1.3.2 Reinforcement Strength

Since the reinforcement strength and spacing are not proportional, a new equation for required reinforcement strength was needed. The analytical equation shown in equation 1 was developed by Wu et al. to incorporate the effect of confinement (i.e., facing rigidity, σ_c), reinforcement spacing, and aggregate size (d_{max}).[10] The equation has been validated against numerous large-scale experiments that were tested to failure (see appendix B). Equation 1 will be discussed in detail in chapter 3.

$$T_{req} = \left[\frac{\sigma_h - \sigma_c}{0.7\left(\frac{S_v}{6d_{max}}\right)}\right] S_v \quad (1)$$

The required reinforcement strength calculated using equation 1 accounts for compaction-induced stresses (CIS), which increase the lateral stress in a GRS mass.[10] CIS are locked in and stiffen the composite. This increased lateral stress must be overcome in order to initiate movement of the GRS mass.

In addition to calculating the required reinforcement strength, a factor of safety (or reduction factor) is necessary to reduce the ultimate strength of the reinforcement used in design. In current design, cumulative reduction factors for geosynthetics made of polypropylene have practically precluded their use in permanent GRS structures.[3] Numerous case histories and field observations have proven, however, that geotextiles can successfully be implemented in several applications, including walls and abutments.[10–13]

Because a GRS structure is a composite mass, the use of cumulative reduction factors for the long-term strength of the reinforcement by itself is unnecessary. A single factor of safety of 3.5 (or resistance factor of 0.4) for ultimate reinforcement strength should be used, which accounts for long-term degradation (creep, durability, and installation damage). This recommended value is derived from the cumulative long-term reduction factors for a GRS mass in conjunction with an overall uncertainty factor of 2.0.[14,10] This factor of safety is based on the results of several tests conducted on different reinforcement materials within soil, including accelerated creep tests.[15]

Note that creep deformation of a GRS wall is the result of soil-geosynthetic interaction. If the backfill has a tendency to creep faster than the geosynthetic reinforcement, the creep rate of the geosynthetic reinforcement will accelerate. Conversely, if the backfill has a tendency to creep slower than the geosynthetic reinforcement, the creep rate of the geosynthetic reinforcement will become smaller. For a GRS wall with a well-compacted granular backfill, the time-dependent deformation will be very small, and the rate of deformation will typically decrease rapidly with time (the geosynthetic cannot creep by itself). This means that creep will cease soon after construction. Moreover, the tensile forces induced in geosynthetic reinforcement at working stresses are typically very small due to stress redistribution. The very small tensile forces also contribute to very small creep deformation. GRS tests have shown that the soil and reinforcement strain together because the lower spacing confines the soil.[14]

For the recommended granular fill, damage to the reinforcement is not a concern.[1] If large aggregate particles (greater than 3 inches in diameter) are used, however, considerable damage to the reinforcement may occur. This would require reevaluation of the combined effects and may necessitate the use of a heavier reinforcement with a greater tensile strength. Such a situation is not discussed in this report.

1.3.3 Reinforcement Length

The base-to-height (B/H) ratio can be reduced to as low as 0.3 as long as external stability is satisfied.[16,17] This is because a GRS mass is freestanding and internally stable. Internally supported systems stabilize a soil mass by the inclusion of the reinforcement alone.[10] Figure 8 shows a stable, internally supported GRS mass without a facing.

Figure 8. Photo. Internally supported GRS structure.

The facing elements of a GRS abutment are not required for structural support and do not carry any appreciable load. GRS facing blocks are primarily a construction aid to provide a form for each lift of compacted fill, a protective barrier, and a façade for aesthetic purposes. To ensure that the face is not loaded, the superstructure is placed with a certain setback and clear space as recommended in the interim implementation manual.[(1)]

CHAPTER 2. NOTATION, ABBREVIATIONS, AND TERMINOLOGY

2.1 NOTATION

γ	Unit weight of soil [F/L^3]
γ_{fb}	Bulk unit weight of facing block [F/L^3]
δ	Friction angle between the geosynthetic and the facing block [rad]
$\Delta\sigma_3$	Change in lateral pressure due to the reinforcement [F/L^2]
ΔS	Differential bridge settlement [L]
ΔS_{abut}	Differential abutment settlement [L]
ΔV_{face}	Volume gained at the face of the GRS mass [L^3]
ΔV_{top}	Volume lost at the top of the GRS mass [L^3]
ε_L	Lateral strain
ε_V	Vertical strain
σ_c	Lateral confining pressure [F/L^2]
σ_h	Lateral pressure [F/L^2]
$\sigma_{h,bin}$	Lateral pressure at the face due to bin pressure [F/L^2]
σ_v	Vertical earth pressure [F/L^2]
f	Soil friction angle [deg]
a_b	Setback distance between the back of the face and the beam seat [L]
b	Bearing width for bridge; beam seat [L]
$b_{q,vol}$	Width of the load along the top of the wall (including the setback) [L]
c	Cohesion [F/L^2]
d_{max}	Maximum grain size [L]
D_f	Depth of facing block unit [L]
D_L	Maximum lateral displacement [L]
D_V	Vertical settlement in the GRS mass [L]
E	Modulus of GRS composite [F/L^2]
F_{bin}	Thrust force found from bin theory [F/L]

H	Height of GRS abutment [L]
K_a	Coefficient of active earth pressure
K_{ar}	Coefficient of active earth pressure for the reinforced backfill
K_{pr}	Coefficient of passive earth pressure for the reinforced backfill
L	Length of the wall [L]
q_b	Equivalent superstructure DL pressure [F/L^2]
q_{calc}	Calculated ultimate capacity [F/L^2]
$q_{measured}$	Measured ultimate capacity [F/L^2]
$q_{rupture}$	Measured vertical capacity at reinforcement rupture [F/L^2]
q_{ult}	Ultimate applied vertical load [F/L^2]
$q_{ult,an}$	Ultimate load-carrying capacity of GRS using the analytical method [F/L^2]
$q_{ult,an,c}$	Ultimate load-carrying capacity of GRS using the analytical method with cohesion [F/L^2]
$q_{ult,emp.}$	Ultimate load-carrying capacity of GRS using the empirical method [F/L^2]
S_v	Reinforcement spacing [L]
T	Reinforcement strength [F/L]
T_{actual}	Actual reinforcement strength at rupture [F/L]
T_{calc}	Calculated reinforcement strength [F/L]
T_f	Ultimate reinforcement strength [F/L]
T_{req}	Required reinforcement strength [F/L]
$T_{req,c}$	Required reinforcement strength including effect of cohesion [F/L]
w	Factor accounting for reinforcement spacing and aggregate size

2.2 ABBREVIATIONS

AASHTO	American Association of State and Highway Transportation Officials
ASD	Allowable Stress Design
CDOT	Colorado Department of Transportation
CIP	Cast-in-place
CIS	Compaction-induced stresses

CMU	Concrete masonry unit
COB	Center of bearing
EDM	Electronic distance measurement
FHWA	Federal Highway Administration
GRS	Geosynthetic Reinforced Soil
GSGC	Generic Soil-Geosynthetic Composite
IBS	Integrated Bridge System
LRFD	Load and Resistance Factor Design
MSE	Mechanically stabilized earth
NCHRP	National Cooperative Highway Research Program
RSF	Reinforced soil foundation
SRW	Segmental retaining wall
TFHRC	Turner-Fairbank Highway Research Center

2.3 TERMINOLOGY

Clear space: The vertical distance between the top of the wall face (block) and base superstructure. Typically, this distance is about 3 inches or at least 2 percent of the wall height.

GRS: Alternating layers of compacted granular fill reinforced with geosynthetic reinforcement (e.g., geotextiles, geogrids). The primary reinforcement spacing in GRS is less than or equal to 12 inches. Facing elements can be frictionally connected to the reinforcement layers to form the outer wall. The facing elements do not need mechanical connections to each other or the layers of reinforcement. The outer wall facing can be built with natural rock, concrete modular block, gabions, timber, or geosynthetic wrapped face. GRS is generic and can be built with any combination of geosynthetic reinforcement, compacted granular fill, and facing system, although some combinations of the three components are more compatible than others.

GRS abutment: A GRS system designed and built to support a bridge. Usually, GRS abutments have three sides: the abutment face wall and two wing walls. All GRS abutments must have the abutment face wall. In some circumstances, depending on the layout, a GRS abutment can be built with one or none of the wing walls.

GRS abutment face wall: The vertical or near vertical wall parallel to the center of bearing and designed to support the bridge. The length of a GRS abutment face wall is typically the total width of the bridge structure plus any additional width necessary to accommodate the structure (e.g., guardrail deflection distance).

GRS-IBS: A unique application of GRS technology in the specific context of bridge abutments. GRS-IBS is different from other, more general GRS abutments that use many common elements associated with traditional bridge abutments. GRS-IBS bridge abutments are built to economically support a bridge on the granular fill directly behind the block face. GRS-IBS can be used to integrate the bridge structure with the bridge approach to create a jointless bridge system. One version of GRS-IBS uses adjacent concrete box beams or void slabs supported directly on the GRS abutments without a concrete footing or elastomeric pads. The bridge has no CIP concrete or approach slab. A typical cross section of IBS shows a GRS mass compacted directly behind the bridge beams to form the approach way and to create a smooth transition from the roadway to the bridge. Another version of GRS-IBS uses steel girders with either a CIP footing or a precast sill. The footing or sill is placed directly on the GRS abutment. The reinforcement layers behind the beam ends are wrapped to confine the compacted approach fill against the beam ends and the adjacent side slopes to prevent lateral spreading. Since the wrapped-face GRS mass behind the beam ends is free standing, the active lateral pressure against the beam ends is considered negligible. The wrapped-face fill also prevents migration of fill during thermal bridge cycles and vehicle live loads.

GRS mass or GRS structure: A composite mass built with GRS that creates a freestanding, internally supported structure with reduced lateral earth pressures with considerable strength. This design permits the use of lightweight modular blocks and the elimination of mechanical connections between blocks and the reinforcement. A GRS mass is not rigid and is therefore tolerant to differential foundation settlement.

GRS wall: Any wall built with GRS.

GRS wing wall: A wall attached and adjacent to the abutment face wall. The wing walls are built at the same time as the abutment face wall and at a right or other angle to the abutment face wall. The wing walls are built to support the roadway and the approach embankment. The wing walls must be designed to retain the soil fill in the core of the approach embankment and to protect the abutment from erosion.

Setback: The lateral distance from the back of the wall face to the front of the bearing area. This distance must be a minimum of 8 inches.

CHAPTER 3. DESIGN METHODOLOGY FOR GRS-IBS

3.1 OVERVIEW OF GRS-IBS DESIGN METHOD

During the past 30 years, GRS technology has been used to build walls, shallow foundations, culverts, bridge abutments, and rock fall barriers. The technology also has been used to stabilize slopes and repair roadways. While GRS technology can provide solutions in a variety of applications and under certain extreme conditions, the design method described in the interim implementation manual provides a recipe for design of GRS-IBS with limitations on abutment heights, bridge spans, and design loads.[1]

The design methods are appropriate for GRS structures (an abutment and wing walls) with a vertical or near vertical face and at a height that does not exceed 30 ft. Although the majority of bridges built with GRS-IBS have spans of less than 100 ft, spans of up to 140 ft have been constructed. While longer spans are possible, the bearing stress on the GRS abutment is limited to 4,000 lb/ft^2. The demands of longer spans on GRS-IBS are not fully understood at this time, and it is recommended that engineers limit bridge spans to approximately 140 ft until further research has been completed.

GRS-IBS abutment capacities are dependent on a combination of the strength of the fill material and the strength of the reinforcement when built in accordance with the two rules of GRS construction: (1) good compaction (95 percent of maximum dry unit weight, according to AASHTO T99) of high-quality granular fill and (2) closely spaced layers of reinforcement (12 inches or less). It is recommended that design or allowable bearing pressure be limited to 4,000 lb/ft^2. For design pressures larger than 4,000 lb/ft^2, the performance criteria must be checked against the applicable stress-strain curve resulting from a performance test. The performance criteria for GRS-IBS consist of a tolerable vertical strain of 0.5 percent and lateral strain of 1 percent. A significant amount of research and practical experience has shown that GRS-IBS designed and constructed within these limits will produce safe, durable systems.

This section focuses on stability within the design method of GRS-IBS.[1] The main distinction with the GRS-IBS design method is the evaluation of internal stability for the GRS abutment, which is different from other reinforced soil systems. External stability in this design method is largely unchanged from other abutment wall systems. However, overturning, or limiting eccentricity, is not a failure mode for fully constructed GRS-IBS.

Two design philosophies are presented in the interim implementation manual: Allowable Stress Design (ASD) and American Association of State and Highway Transportation Officials (AASHTO) Load and Resistance Factor Design (LRFD).[1] It is FHWA policy that design for Federal-aid funded projects be conducted using the LRFD methodology. The LRFD format presented was normalized to produce the same results as the ASD method and does not represent a statistically based calibration that would be consistent with other LRFD-based methods. After sufficient data are produced and collected as a result of this technology deployment and other efforts, a thorough statistical analysis will be performed to appropriately produce LRFD specifications for the design of GRS-IBS.

3.2 EXTERNAL STABILITY

A GRS abutment is a type of gravity structure. Therefore, external stability should be evaluated for the direct sliding, bearing capacity, global stability, and overturning failure modes limiting this type of construction. However, because a GRS mass is relatively ductile and free of tensile strength, overturning about the toe, in a strict sense, is not a possible response to earth pressures at the back of the mass or loading on its top. Other attributes of GRS-IBS also tend to preclude overturning as a mode of failure. GRS-IBS consists of two abutments supporting an integrated superstructure that would function as a strut to resist overturning, and each GRS mass has a reinforced integration zone above its heel, also resisting the overturning mode of failure. Consequently, while direct sliding, bearing capacity, and global stability are evaluated in conventional ways, overturning is sometimes addressed by inspection and comparison to observations of past performance.

Observations of past performance show that the flexible, internally stabilized soil mass of GRS-IBS construction, in combination with an RSF, results in more uniform stress distribution, resisting any applied vertical and lateral loads. Observations also show that, in addition to lack of overturning, the combination of vertical and lateral loads, as limited by analysis of direct sliding, bearing capacity, and global stability, does not cause excessive deformation at the face of the GRS mass or other undesirable performance.

While this combination of unique features and behavior eliminates the need to analyze overturning as a failure mode for completed GRS-IBS, the engineer may choose to analyze for overturning during an intermediate phase of construction with consideration for the time needed for an overturning mechanism to develop and the concurrent level of loading or for project configurations different from those described herein. For example, overturning may still be a viable failure mode for abutment wing walls constructed with GRS technology if they retain soil other than reinforced soil from the abutment or opposite wing wall (i.e., if they retain natural soil).

3.3 INTERNAL STABILITY

Internal stability for a GRS abutment consists of evaluating ultimate capacity, deformations, and required reinforcement strength. There are two approaches to internal stability: empirical and analytical. Empirically, an engineer can predict the ultimate capacity and the deformations of a GRS abutment. Analytically, an engineer can estimate the ultimate capacity and the required reinforcement strength.

Connection strength and pullout are not evaluated in the design of the GRS-IBS as they are with other reinforced soil systems. The design of GRS structures assumes a relatively constant earth pressure with depth at the wall face (see figure 9). This method takes into account the tensile forces in the reinforcement, which counteract the classical lateral earth pressure distribution. This occurs because the reinforcement, not the wall face, acts to restrain lateral deformation of the soil.

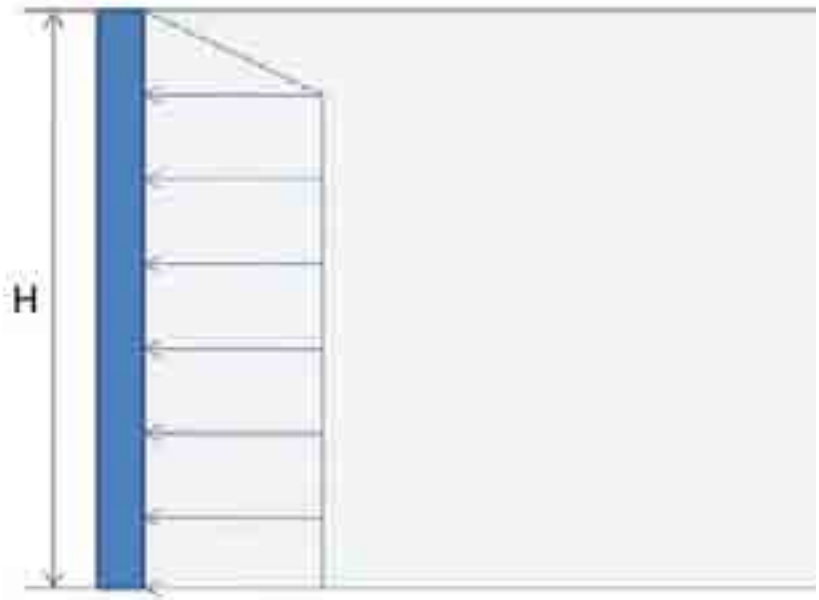

Figure 9. Illustration. Idealized lateral earth pressure at the face of a GRS structure.

Wu et al. proposed that the lateral pressure distribution between reinforcements is based on the concept of bin pressure.[11] In an idealized bin pressure diagram, the pressure is zero at the depth of any reinforcement layer within a bin. The lateral earth pressure increases linearly with depth before decreasing to zero at the next reinforcement layer. Because reinforcement may deform slightly and the interface between the soil and reinforcement may not be perfectly bonded, the bin pressure diagram shown in figure 10 was developed.[11] The bin pressure is not a function of wall height. Instead, the bin pressure is only a function of reinforcement spacing and the strength parameters of the soil (see equation 2).

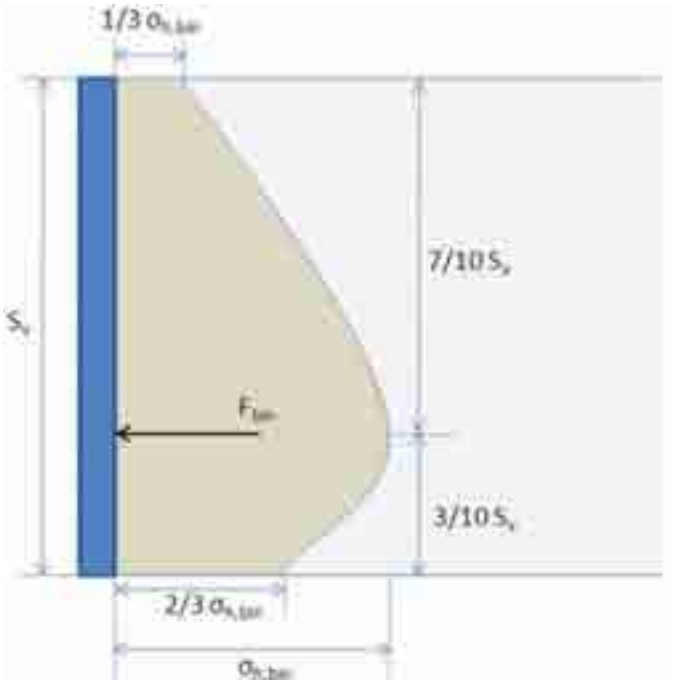

Figure 10. Illustration. Bin pressure diagram for GRS structures.[11]

$$F_{bin} = 0.72\gamma K_a S_v^2 \quad (2)$$

The thrust force against the wall face calculated using equation 2 is lower than that using the theory of active earth pressure. This eliminates the need for mechanical connections between the wall face and the reinforcement. A frictional connection, recommended in GRS design, is sufficient to prevent connection failure. The facing blocks sit directly on the reinforcing geosynthetic and are held in place purely by the friction between the reinforcement and the concrete block. This is an adequate connection because the GRS is internally supported by the closely spaced reinforcement and does not need the facing block to resist lateral pressures. As such, connection strength is not an internal stability problem in GRS design. Nevertheless, the capacity of this simple method of connection is reported in appendix A.

In a GRS structure, there is no thrust on the wall face due to surcharge or bridge loads. This is because the GRS mass is internally supported by the closely spaced reinforcement layers of the bearing reinforcement bed. Because the facing elements (e.g., concrete masonry unit (CMU) blocks) are frictionally connected and the bulk unit weight of the facing is smaller or about the same as that of the GRS mass, the reinforcement, soil, and facing elements all strain together. The interaction between the reinforcement and the soil is such that the soil is strong in compression while the reinforcement provides the tensile capacity, creating the composite mass. Any thrust that occurs due to the surcharge and bridge loads is absorbed to some extent by the reinforcement and does not transmit to the face.

3.3.1 Ultimate Capacity

The ultimate vertical capacity of a GRS mass is found either empirically or analytically. It is recommended that the ultimate capacity be found empirically, if possible. A performance test should be conducted to determine the ultimate capacity empirically if the reinforced fill is different from the reported performance test in this report. Testing will provide the most accurate results for the design. If a performance test cannot be performed, the analytical method can be used to determine the ultimate capacity.

3.3.1.1 Empirical Method

Empirically, the results of an applicable performance test using the same geosynthetic reinforcement and compacted granular backfill as planned for the site should be used. The *ultimate vertical capacity* in this case is defined as the stress at which the performance test mass strains 5 percent vertically. Several performance tests have been conducted with different materials, as shown in figure 11. In all examples, the facing elements were frictionally connected to the GRS mass.

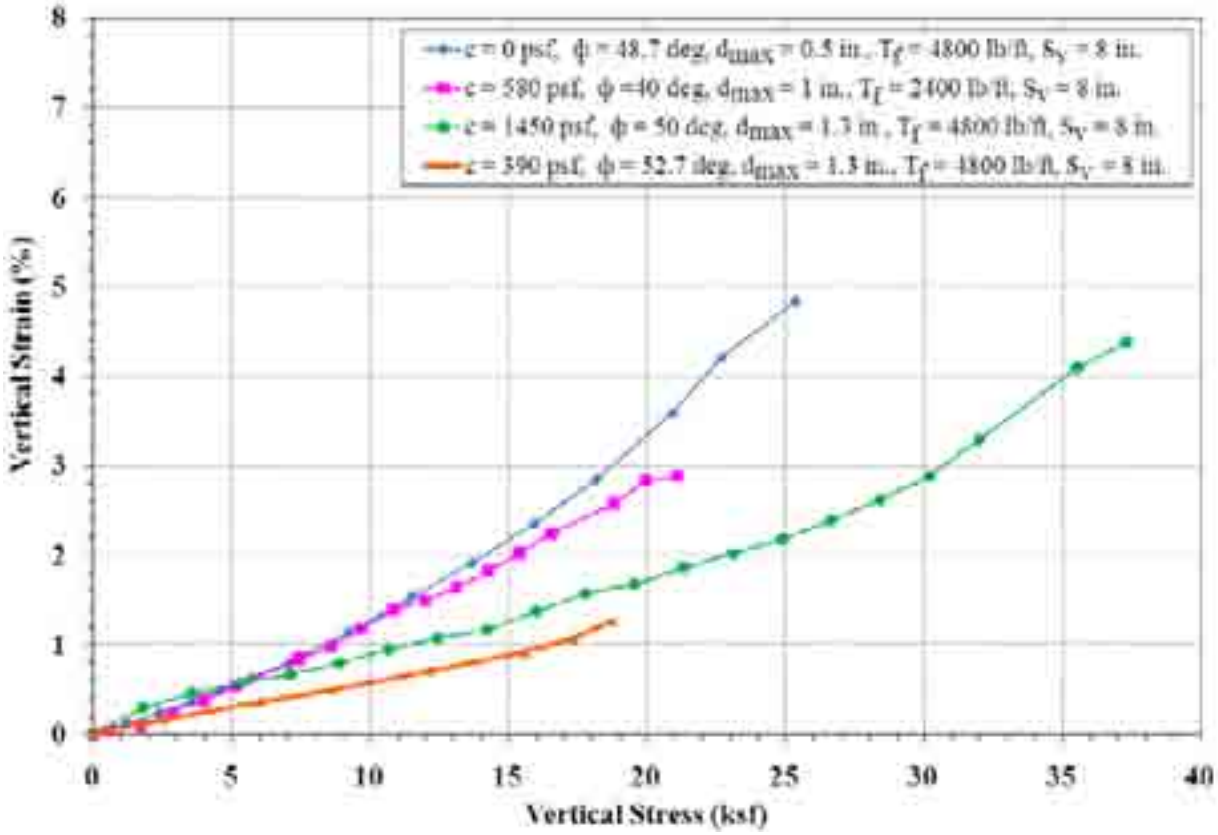

Figure 11. Graph. Performance test results for different materials.

Note that three of the materials in figure 11 have cohesion (*c*). Relatively clean granular fills (sands, gravels, and rock fills) share two common characteristics in terms of Mohr-Coulomb strength parameters: (1) no cohesion and (2) a curved failure envelope over a wide range of confining pressure. Depending on how the strength parameters are evaluated, one may come up with a set of *c* and f values for a granular soil. The cohesion should be ignored in design if it will not be there during the service life of the structure. Cohesion may be apparent (due to capillary tension in a moist soil that will vanish when wetted or dry) or the small amount of clay binder may disappear when the granular soil becomes submerged for a while. If this is the case, refer to the analytical method that ignores the effect of cohesion.

3.3.1.2 Analytical Method

The load-carrying capacity of a GRS wall and abutment ($q_{ult,an,c}$) can be evaluated using an analytical formula (see equation 3).[10] The analytical formula was originally developed for GRS walls, but it is also applicable to GRS abutments. Note that the analytical method assumes that the backfill satisfies the criteria outlined in the interim implementation manual.[1]

$$q_{ult,an,c} = \left[\sigma_c + 0.7^{\left(\frac{S_v}{6d_{max}}\right)}\frac{T_f}{S_V}\right]K_{pr} + 2c\sqrt{K_{pr}} \quad (3)$$

Where σ_c is the lateral confining pressure, S_v is the reinforcement spacing, d_{max} is the maximum grain size of the reinforced backfill, T_f is the ultimate strength of the reinforcement, and K_{pr} is

the coefficient of passive earth pressure for the reinforced fill. For a GRS wall with dry-stacked modular block facing, the value of σ_c can be estimated according to equation 4.

$$\sigma_c = \gamma_{fb} D_f tan\delta \quad (4)$$

Where γ_{fb} is the bulk unit weight of the facing block, D_f is the depth of the facing block unit (in the direction perpendicular to the wall face), and δ is the friction angle between the geosynthetic reinforcement and the top or bottom surface of the facing block.

The ultimate capacity ($q_{ult,an,c}$) was determined using Bell's relation for lateral earth pressure, shown in equation 5.[18] The equation was then rearranged to solve for the vertical pressure (σ_v).

$$\sigma_h = \sigma_v K_a - 2c\sqrt{K_a} \quad (5)$$

Where σ_h is the lateral earth pressure (see equation 6), σ_v is the vertical pressure, K_a is the active earth pressure coefficient, and c is the cohesion.

$$\sigma_h = \sigma_c + \Delta\sigma_3 \quad (6)$$

Where σ_c is the lateral confining pressure (equation 4) and $\Delta\sigma_3$ is the change in lateral pressure due to the reinforcement (see equation 7).

$$\Delta\sigma_3 = w\frac{T}{S_v} \quad (7)$$

Where w is a factor accounting for the effect of reinforcement spacing and aggregate size (see equation 8), T is the reinforcement strength, and S_v is the reinforcement spacing.

$$w = 0.7^{\frac{S_v}{6d_{max}}} \quad (8)$$

Where S_v is the reinforcement spacing and d_{max} is the maximum aggregate size. The w factor was determined based on several large-scale GRS experiments.[10] Inputting the ultimate strength of the reinforcement (T_f) for the reinforcement strength (T) in equation 7 and solving equation 5 for the vertical pressure (σ_v) will yield the ultimate capacity of the GRS abutment (equation 3).

Figure 12 shows the predictive capability of equation 3, where the calculated ultimate load-carrying capacity is compared to measured values for a number of full-scale experiments and in-service GRS structures. The complete set of data, showing the range of fills, reinforcement strength, and spacing, can be found in appendix B. Note that equation 3 should not be used in design.

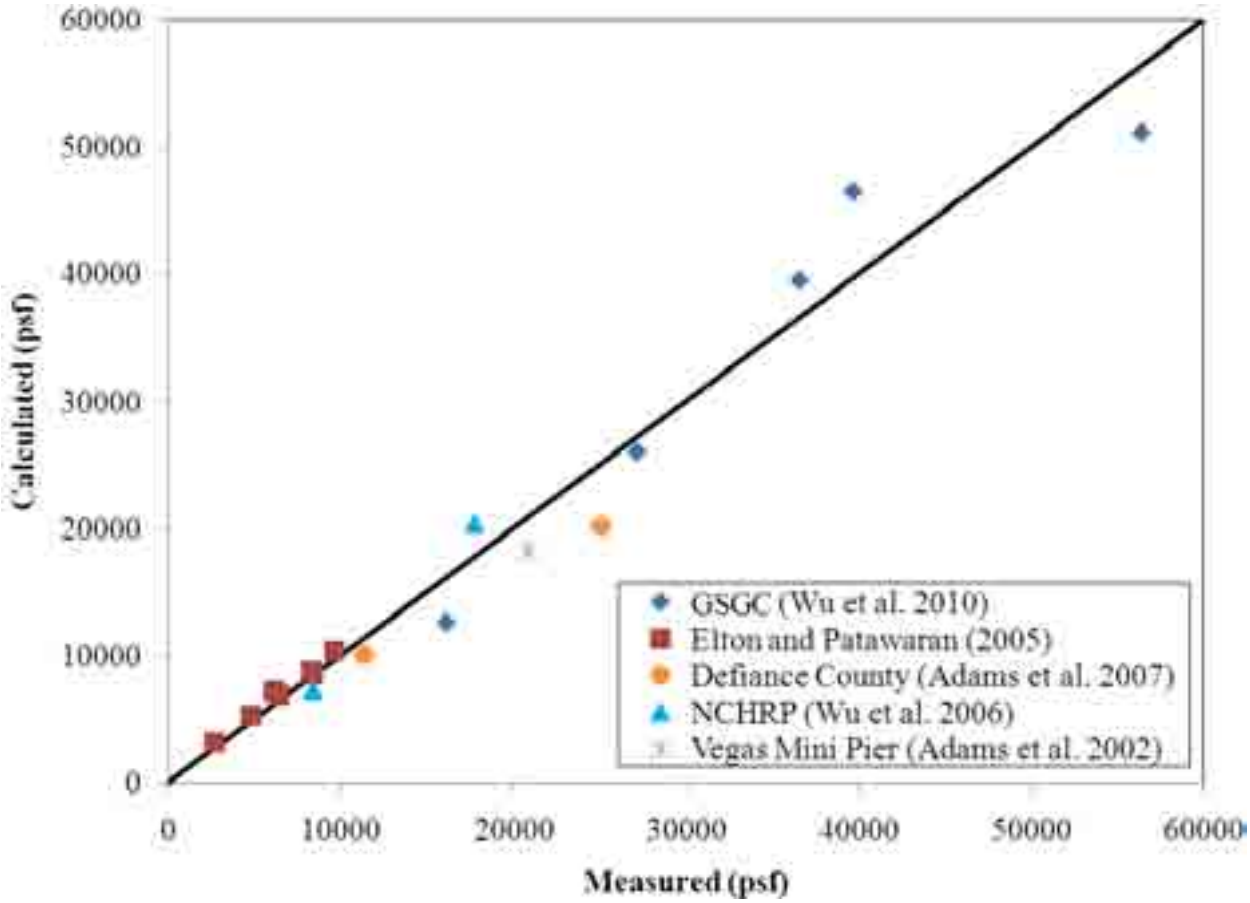

Figure 12. Graph. Predictive capability of the soil-geosynthetic composite capacity equation.

To estimate the ultimate capacity used in design, equation 3 is modified to neglect confining stress (σ_c) and cohesion (c) and is referred to as the soil-geosynthetic composite capacity equation (see equation 9).[1,10] The magnitude of σ_c is typically very small and should conservatively be assumed to equal zero. The effect of cohesion is also removed in design as it cannot be counted on in the long-term strength of the GRS abutment.

$$q_{ult,an} = \left[0.7^{\left(\frac{S_v}{6d_{max}}\right)} \frac{T_f}{S_v}\right] K_{pr} \quad (9)$$

Where S_v is the reinforcement spacing, d_{max} is the maximum grain size of the reinforced backfill, T_f is the ultimate strength of the reinforcement, and K_{pr} is the coefficient of passive earth pressure for the reinforced fill.

3.3.2 Deformations

The vertical deformation involves empirically finding the strain from an applicable performance test curve. The lateral strain is then analytically found assuming the theory of zero volume change.

3.3.2.1 Vertical

The vertical strain of the GRS mass is found from the intersection of the applied vertical stress due to the dead load (q_b) and the stress-strain curve found from a performance test (see figure 13). The vertical strain should be less than about 0.5 percent. The vertical deformation, or settlement, of the GRS abutment is the vertical strain multiplied by the height of the wall or abutment. Because the GRS abutment is built with a granular fill, the majority of settlement within the GRS mass will occur immediately after the placement of dead loads (q_b) and before the bridge is opened to traffic.

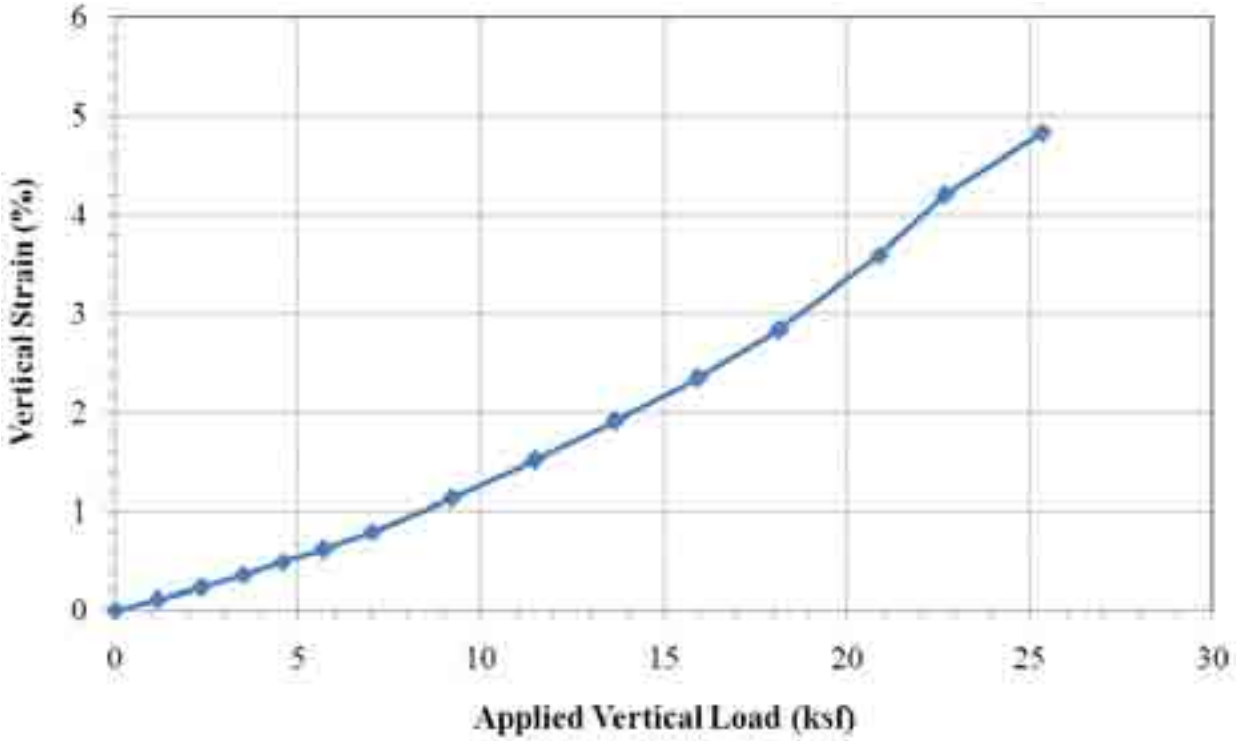

Figure 13. Graph. Design envelope for vertical strain at 8-inch reinforcement spacing.

The settlement of the underlying foundation soils is determined separately using classic soil mechanics theory for immediate (elastic) or consolidation settlement. Factors such as excavation and the RSF should be taken into account, because the removal of overburden relieves stress on the foundation soil. Settlement of the foundation soil can be calculated using the FHWA *Soils and Foundations Reference Manual*.[(19)]

Figure 14 shows the results of the previously described method for five in-service GRS abutment walls in Defiance County, OH. The measured vertical strain at the applied dead loads fits well with the curve. More information on these five structures is given in chapter 4.

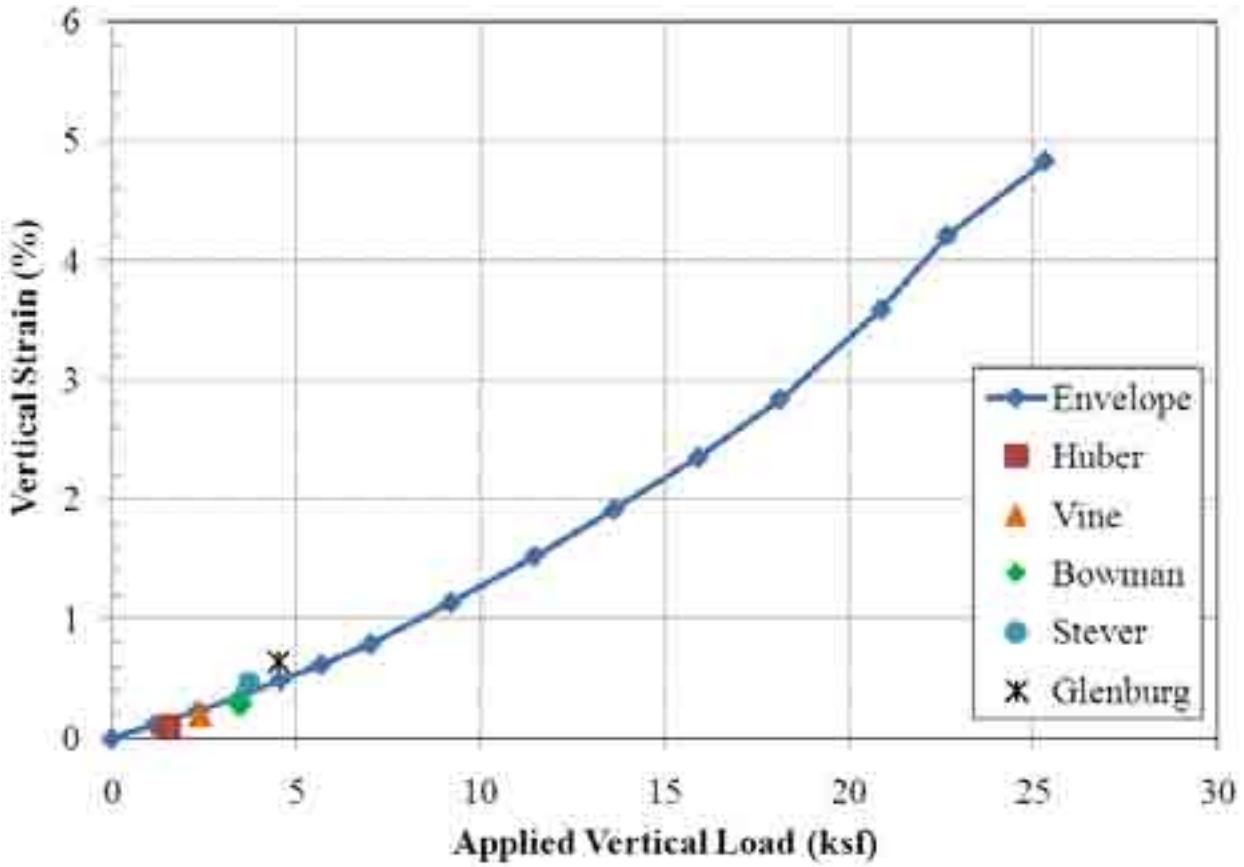

Figure 14. Graph. Deformation estimation from in-service GRS-IBS structures.

3.3.2.2 Lateral

In response to a vertical load, the composite behavior of a properly constructed GRS mass is such that both the reinforcement and soil strain laterally together. This fact can be used to predict both the maximum lateral reinforcement strain and the maximum face deformation at a given load. The method conservatively assumes a zero volume change in the GRS mass and represents a worst-case scenario. The maximum lateral displacement of the abutment face wall can be estimated using the following procedure.[20]

Assuming a uniformly loaded vertical wall in plane strain conditions (such as with a strip footing), the maximum lateral displacement (D_L) occurs in one direction along one wall face (see figure 15). It is found by assuming the volume lost at the top (ΔV_{top}) due to settlement is equal to the volume gained at the face (ΔV_{face}) due to lateral deformation (see equation 10).

$$\Delta V_{top} = b_{q,vol} L D_v = \Delta V_{face} = \frac{1}{2} H L D_L \quad (10)$$

Where $b_{q,vol}$ is the width of the load along the top of the wall including the setback, L is the unit length of the wall, D_v is the vertical settlement in the GRS mass, and H is the wall height. Equation 10 can then be solved for the maximum lateral displacement (see equation 11). The lateral strain (ε_L) is then found using equation 12. The lateral strain should be limited to around 1 percent.

$$D_L = \frac{2b_{q,vol}\,D_v}{H} \tag{11}$$

$$\varepsilon_L = \frac{D_L}{b_{q,vol}} = \frac{2D_v}{H} = 2\varepsilon_v \tag{12}$$

Where ε_V is the vertical strain at the top of the wall. Equation 10 comes from the assumptions of a triangular lateral deformation and a uniform vertical deformation. Note that the location of the maximum lateral deformation depends on the loading and fill conditions, but the volume gained will still equal the volume lost at the top.

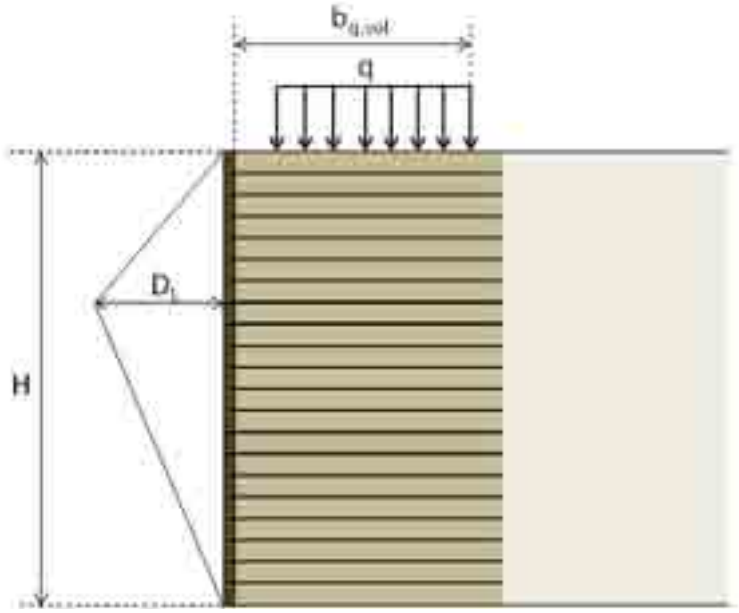

Figure 15. Illustration. Lateral deformation of a GRS structure.

3.3.3 Required Reinforcement Strength

The required reinforcement strength in the direction perpendicular to the wall face ($T_{req,c}$) can be determined analytically using equation 13. Note that equation 13 is equation 3 rearranged to solve for the required reinforcement strength to prevent failure. In the design, the effect of confinement (σ_c) and cohesion (c) are ignored to find the required reinforcement strength (T_{req}) to ensure long-term strength and durability (see equation 14).

$$T_{req,c} = \left[\frac{\sigma_h - \sigma_c - 2c\sqrt{K_{ar}}}{0.7\left(\frac{S_v}{6d_{max}}\right)}\right] S_v \tag{13}$$

$$T_{req} = \left[\frac{\sigma_h}{0.7\left(\frac{S_v}{6d_{max}}\right)}\right] S_v \tag{14}$$

Where σ_c is the lateral confining pressure of GRS mass (equation 4), assumed to equal zero for a CMU block face wall; S_v is the reinforcement spacing; d_{max} is the maximum grain size of backfill; K_{ar} is the active earth pressure coefficient for the reinforced fill; and σ_h is the total lateral stress within the GRS mass at a given depth and location.

Equation 13 was validated by comparing it to the measured reinforcement strength at failure, as shown in figure 16. The required reinforcement strength at failure matches well with the actual values of strength at rupture. The input data for each case in figure 16 are shown in appendix B.

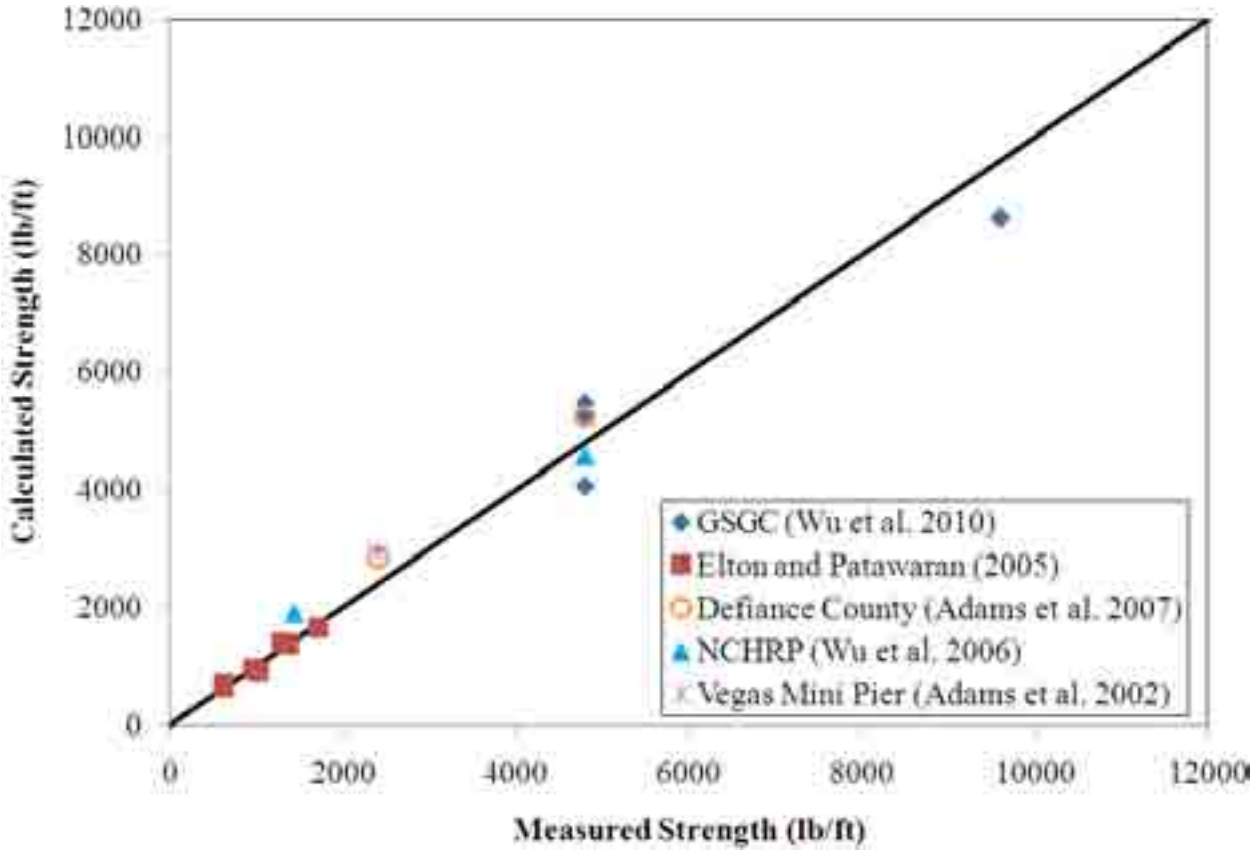

Figure 16. Graph. Predictive capability of the required reinforcement strength equation.

CHAPTER 4. CASE HISTORIES

4.1 INTRODUCTION

This chapter presents the performance of in-service GRS abutments, specifically, bridges built with GRS-IBS between 2005 and 2010. The performance of the first series of GRS-IBS indicates that the method has considerable potential to advance the state of the practice. Included in this chapter is a performance overview of several other bridges built with GRS abutments in the private and public sectors within the United States and Canada. The chapter also lists various case histories of many GRS walls built during the past 20 years to validate the long-term performance of these structures.

The elimination of the joint at the bridge ends helps improve the durability of both the beam ends and the bearings in conventional bridge systems. A distinctive feature in the design of GRS-IBS is that it works with settlement instead of resisting it to create a compatible connection between the approach and the road, hopefully as a long-term solution to the bump at the end of the bridge. Reducing the bump at the end of bridge will improve the bridge's overall performance and serviceability. The bump not only creates a chronic maintenance issue but also induces an amplification of live load on the superstructure, creating fatigue on bridge elements.

4.2 DEFORMATIONS

The performance of nearly 20 bridges built with GRS-IBS has been an improvement on similar bridges built with conventional construction techniques. The GRS-IBS bridges have performed as well as conventional bridges structurally and functionally in addition to eliminating the bump at the end of the bridge that often results from conventional construction. At the time of this report, the suppression of the bump had been maintained for all in-service GRS-IBS bridges. The first bridge constructed with the IBS method, Bowman Road Bridge, has been in service since 2005 without the development of a crack in the asphalt layer from the road to the bridge.

Of the nearly 30 bridges built with GRS-IBS, 5 bridges have current data from monitoring of settlement at the abutments. The total settlement and deformation (and, thus, vertical strain) of the GRS abutment due the bridge load is recorded using either a standard survey level and rod system or an electronic distance measurement (EDM) survey referenced off a permanent survey pole and benchmarks. The methods to monitor performance are discussed in detail in the interim implementation manual.[(1)]

In both methods, settlement is recorded for both the abutment face wall and the superstructure. The difference between the settlement measured on the abutment face wall and on the superstructure is the vertical deformation within the GRS mass due to the bridge load. This value can be divided by the height of the abutment face wall to compute the vertical strain within the GRS abutment. The lateral strain and deformation can then be estimated.

4.2.1 Vertical Deformation

Table 2 gives general information about five bridges built using GRS-IBS. The settlement of three of the bridges, Vine Street, Glenburg Road, and Huber Road, was monitored with the survey level system over the course of 3.2, 3.6, and 2.4 years, respectively (see figure 17 through figure 22).

Lateral deformation was not measured on these bridges, but it can be estimated knowing the vertical deformation (see chapter 3).

Table 2. Bridge information summary.

Bridge	Date Built	Abutment	Abutment Height (ft)	Dead Load (kips/ft^2)	Span Length (COB to COB) (ft)	Width of Bridge (ft)
Vine Street	October 2006	North	12.36	2.37	50.0	32.67
		South	10.36			
Glenburg Road	May 2006	North	13.22	4.53	30.6	28
		South	12.80			
Huber Road	August 2007	North	17.30	1.53	28.0	28
		South	16.16			
Bowman Road	October 2005	East	16.91	3.46	79.0	34
		West	16.47			
Tiffin River	July 2009	North	20.52	3.69	134.0	36
		South	18.00			

COB = Center of bearing.

Figure 17. Photo. Vine Street Bridge.

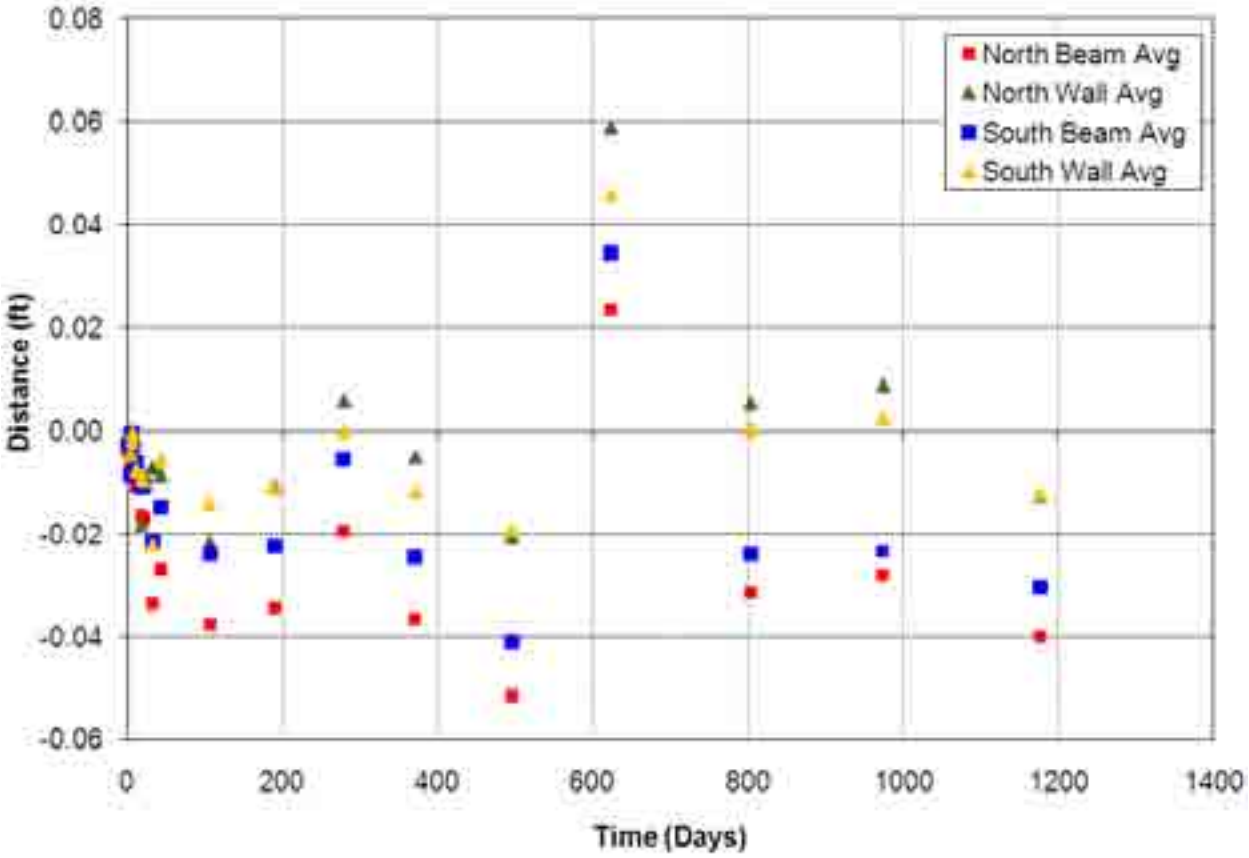

Figure 18. Graph. Vine Street GRS-IBS settlement versus time.

Figure 19. Photo. Glenburg Road Bridge under flood conditions.

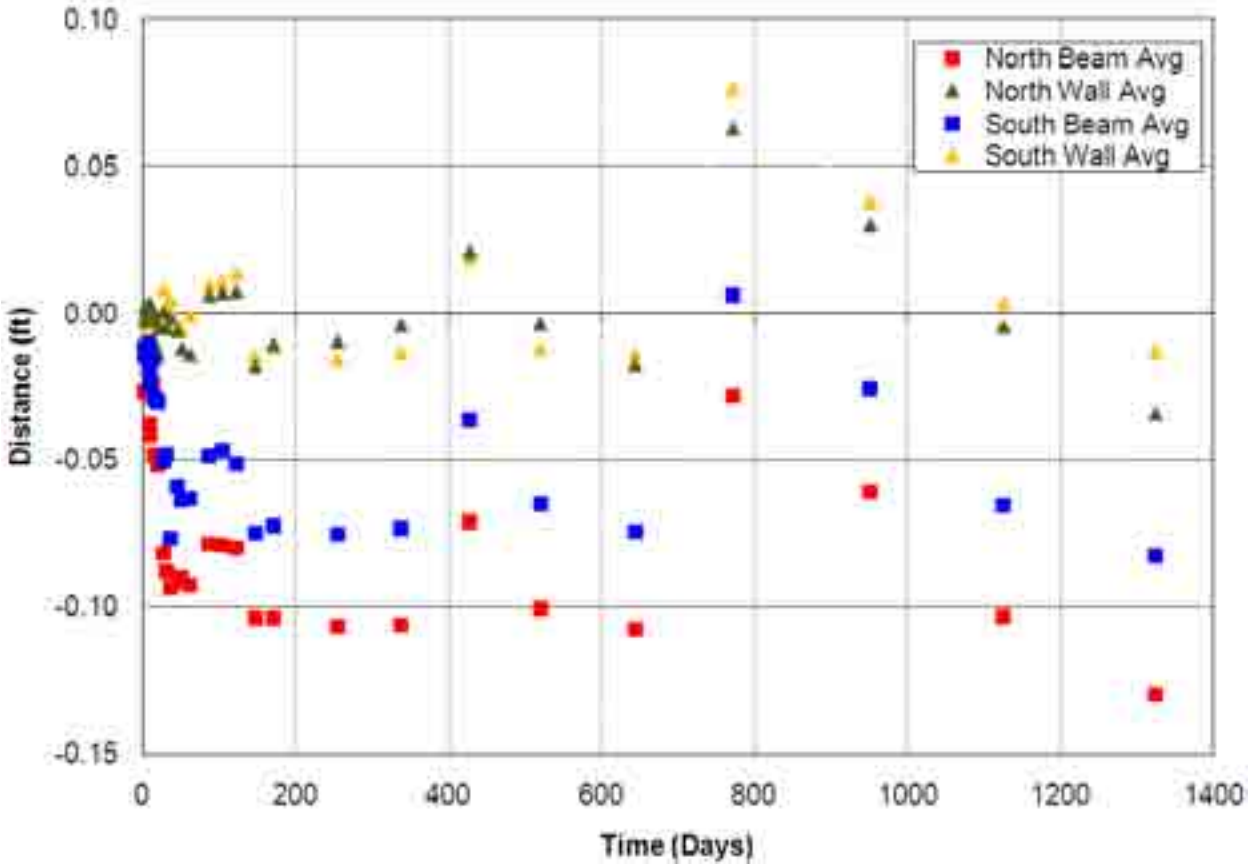

Figure 20. Graph. Glenburg Road GRS-IBS settlement versus time.

Figure 21. Photo. Huber Road Bridge.

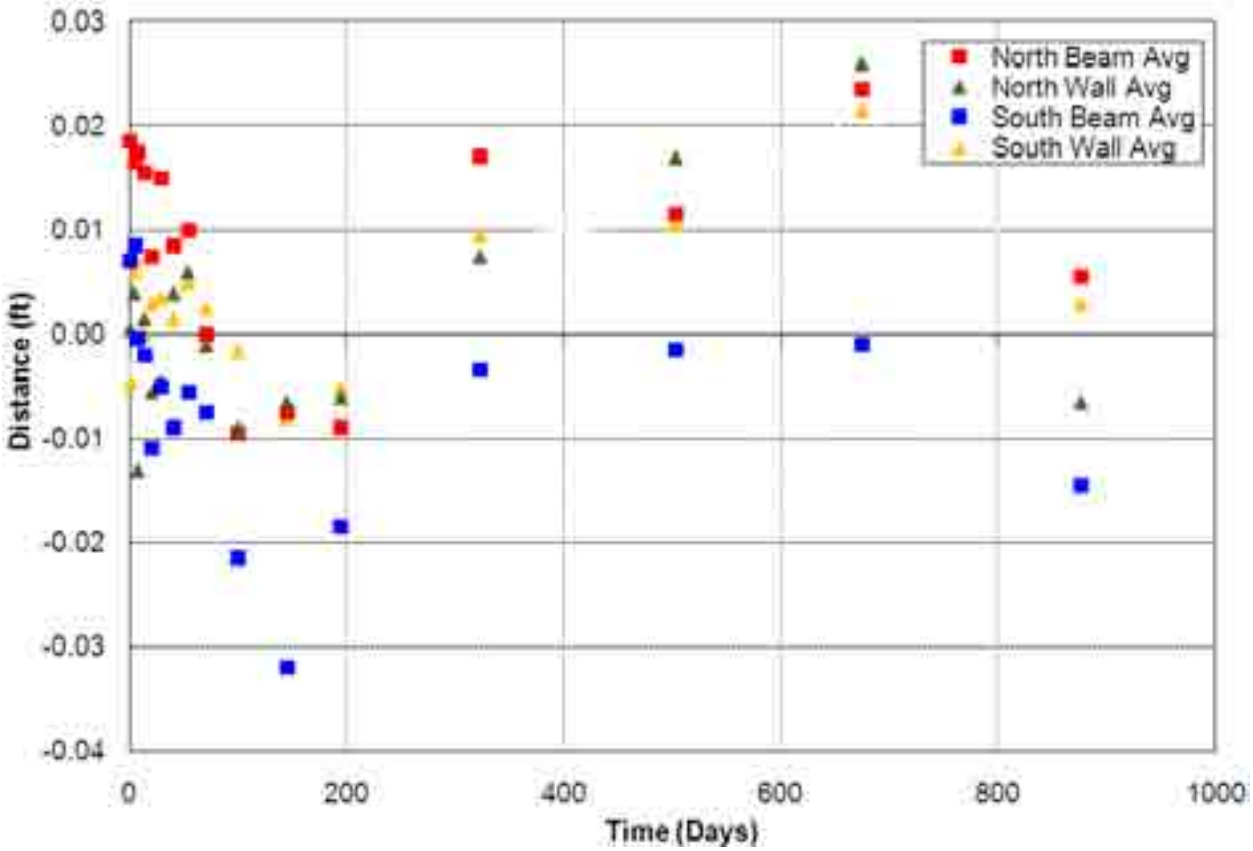

Figure 22. Graph. Huber Road GRS-IBS settlement versus time.

The settlement of two of the bridges, Bowman Road and Tiffin River, was monitored with the EDM and total station system over the course of 1.5 years (see figure 23 through figure 26). Lateral deformation was also recorded using this method for both bridges, but the noise level on Bowman Road Bridge was considered too high to be of any significant use.

Figure 23. Photo. Bowman Road Bridge after 4.5 years.

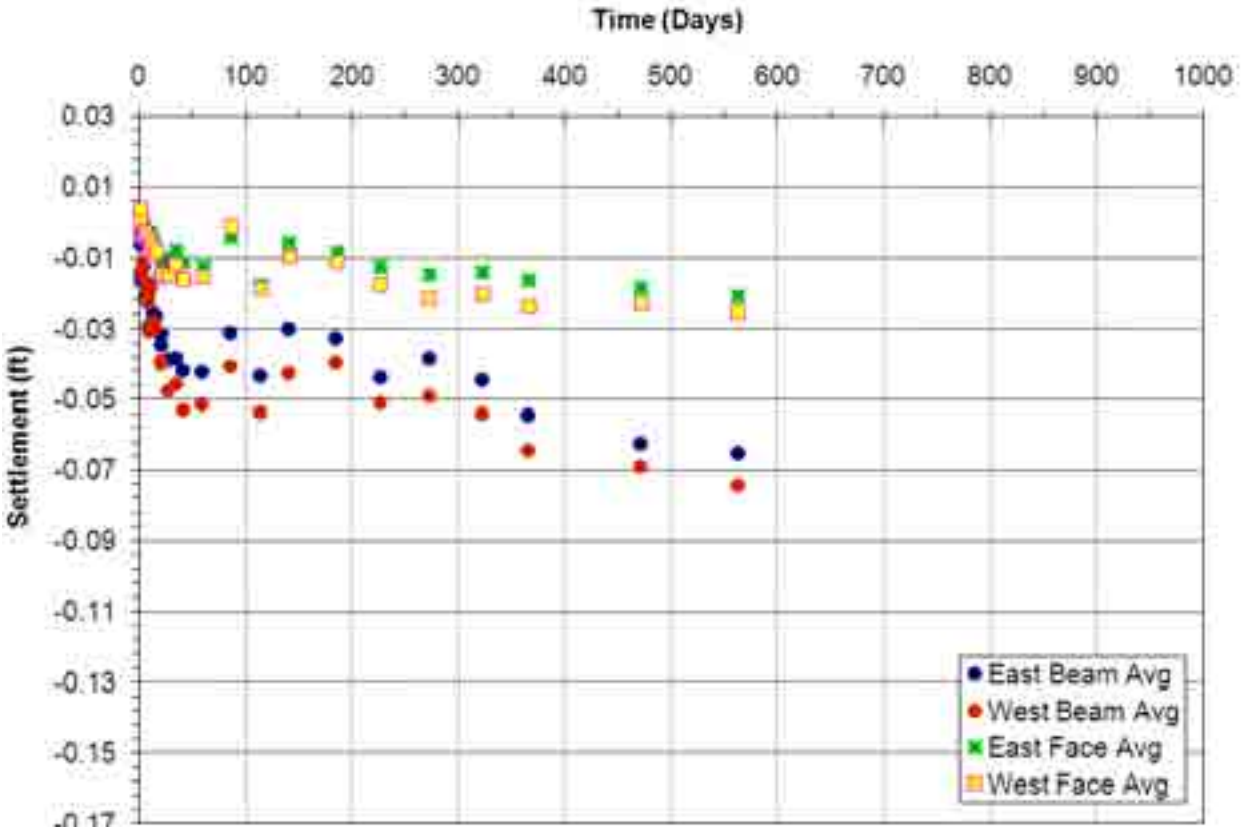

Figure 24. Graph. Bowman Road GRS-IBS settlement versus time.

Figure 25. Photo. Tiffin River Bridge.

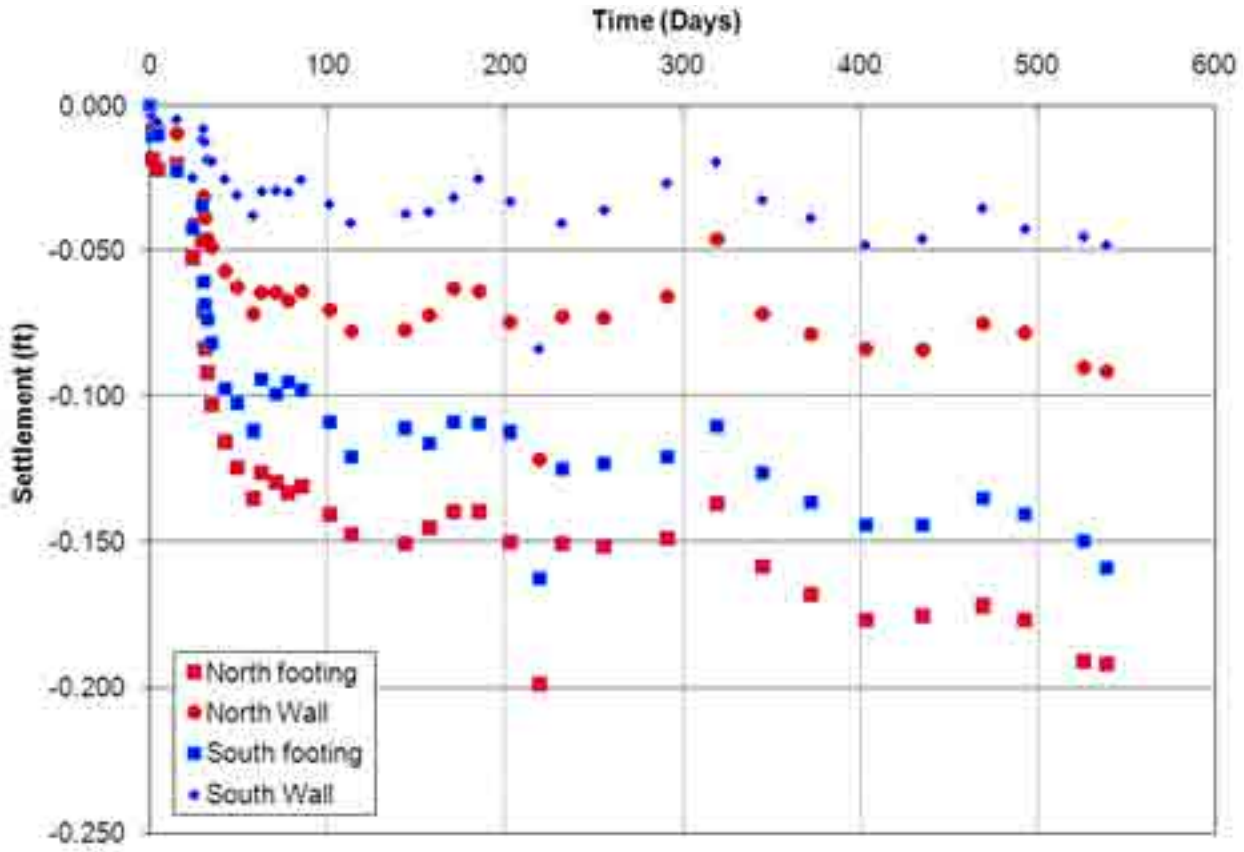

Figure 26. Graph. Tiffin River GRS-IBS settlement versus time.

For the majority of these cases, the bridges were built with concrete box beams, so the settlement was essentially instantaneous with one large load increment. The settlement history for Tiffin River Bridge, shown in figure 26, is slightly different than the settlement of the other bridges because the bridge was assembled in stages. The record began following the erection of the steel girders on day 0. The plot clearly shows the settlement due to the weight of the concrete deck (installed on day 30). The bridge was opened to traffic on day 60, but this is not apparent in the settlement record. The postconstruction settlement, from when the Tiffin River Bridge was opened to traffic until the last settlement reading, was 0.023 ft on the north abutment and 0.027 ft on the south abutment. Compared to the settlement due to casting the concrete deck (0.079 and 0.06 ft for the north and south abutments, respectively), the settlement after traffic is minimal and reaches the secondary settlement stage. In fact, in all of the bridges, the primary settlement essentially ceased before the bridges opened to traffic.

The differential settlement for an individual abutment, the uniformity of abutment settlement, the differential settlement between opposite abutments (i.e., bridge differential settlement), and the angular distortion were calculated for each of the five bridges (see table 3). The total vertical settlement and strain (including the GRS abutment and the foundation settlement) along with just the GRS abutment settlement and strain are shown in table 4.

Table 3. Movement information for five bridges.

Bridge	Abutment	Abutment Height (ft)	Abutment Differential Settlement (ΔS_{abut}) (ft)	Uniformity of Abutment Settlement (ΔS_{abut}/ width of bridge)	Bridge Differential Settlement (ΔS) (ft)	Angular Distortion (ΔS/ span length)
Vine Street	North	12.36	0.024	0.0007	0.009	0.00018
	South	10.36	0.015	0.0005		
Glenburg Road	North	13.22	0.020	0.0006	0.012	0.00039
	South	12.80	0.008	0.0002		
Huber Road	North	17.30	0.011	0.0004	0.01	0.00036
	South	16.16	0.021	0.0008		
Bowman Road	East	16.91	0.022	0.0007	0.019	0.00024
	West	16.47	0.003	0.0001		
Tiffin River	North	20.52	0.003	0.0001	0.033	0.00025
	South	18.00	0.005	0.0003		

Table 4. Vertical settlement and strain information for five bridges.

Bridge	Average Abutment Height (ft)	Average Total Settlement (ft)	Average Total Vertical Strain (percent)	Average GRS Settlement (ft)	Average GRS Vertical Strain (percent)
Vine Street	11.36	-0.035	0.31	0.023	0.20
Glenburg Road	13.01	-0.107	0.82	0.083	0.64
Huber Road	16.73	-0.004	0.024	0.015	0.09
Bowman Road	16.69	-0.07	0.42	0.047	0.28
Tiffin River	19.26	-0.175	0.91	0.106	0.55

The long-term settlement can be forecasted by plotting the secondary settlement in log-time scale. For example, the settlement of Bowman Road Bridge is plotted in log-time scale with the appropriate trend lines included in figure 27. After 100 years (the service life of the bridge), the average predicted creep settlement is 0.09 ft for the bridge and 0.035 ft for the abutment walls. The difference between these two values, 0.055 ft, represents the creep settlement of the GRS abutment alone after 100 years.

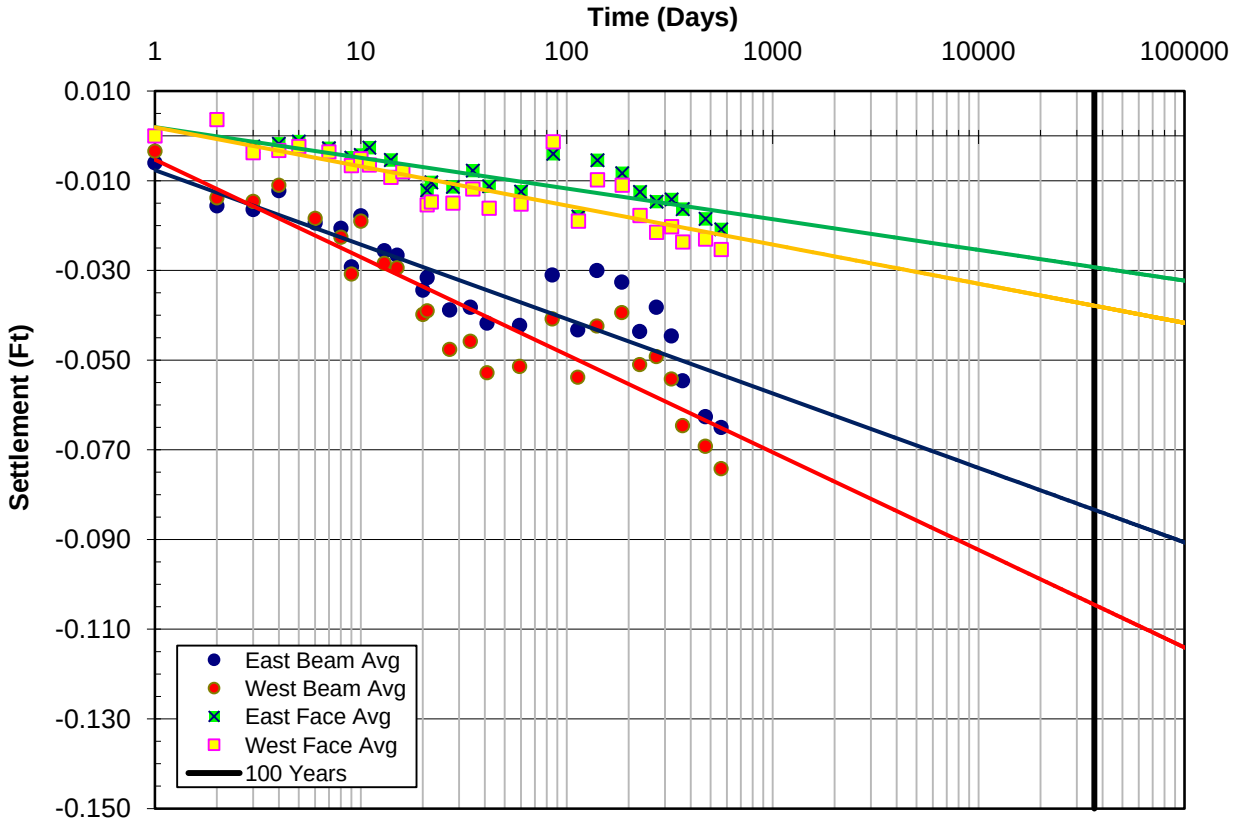

Figure 27. Graph. Settlement versus log-time to predict creep settlement for the Bowman Road Bridge at 100 years.

Another example comes from a long-term settlement study of a GRS-IBS structure built at FHWA's Turner-Fairbank Highway Research Center (TFHRC). This 12-year settlement study represents the longest settlement record of a GRS abutment. Within the embankment, a tunnel was constructed to serve several purposes, including measuring deformation, observing the versatility of GRS, understanding reinforcement strength on deformation, and providing a walkway to move people and equipment through the embankment (see figure 28 and figure 29). The overburden on the tunnel is equal to about 3,800 lb/ft^2, about the same as a typical bridge load.

Figure 28. Photo. GRS-IBS tunnel at TFHRC.

Figure 29. Photo. Close-up of GRS-IBS tunnel at TFHRC.

Settlement was measured on both sides of the tunnel wall: the abutment side and the embankment side. Each side of the wall had different reinforcement strengths. The abutment side was reinforced with 4,800 lb/ft geotextile, and the embankment side was reinforced with 2,100 lb/ft geotextile. The measurements over 12 years show that the side with 4,800 lb/ft reinforcement has settled about the same as the side with 2,100 lb/ft reinforcement (see figure 30). The settlement difference between the two sides is only about 0.0024 ft. The fabric strength did not play a role in the GRS deformation.

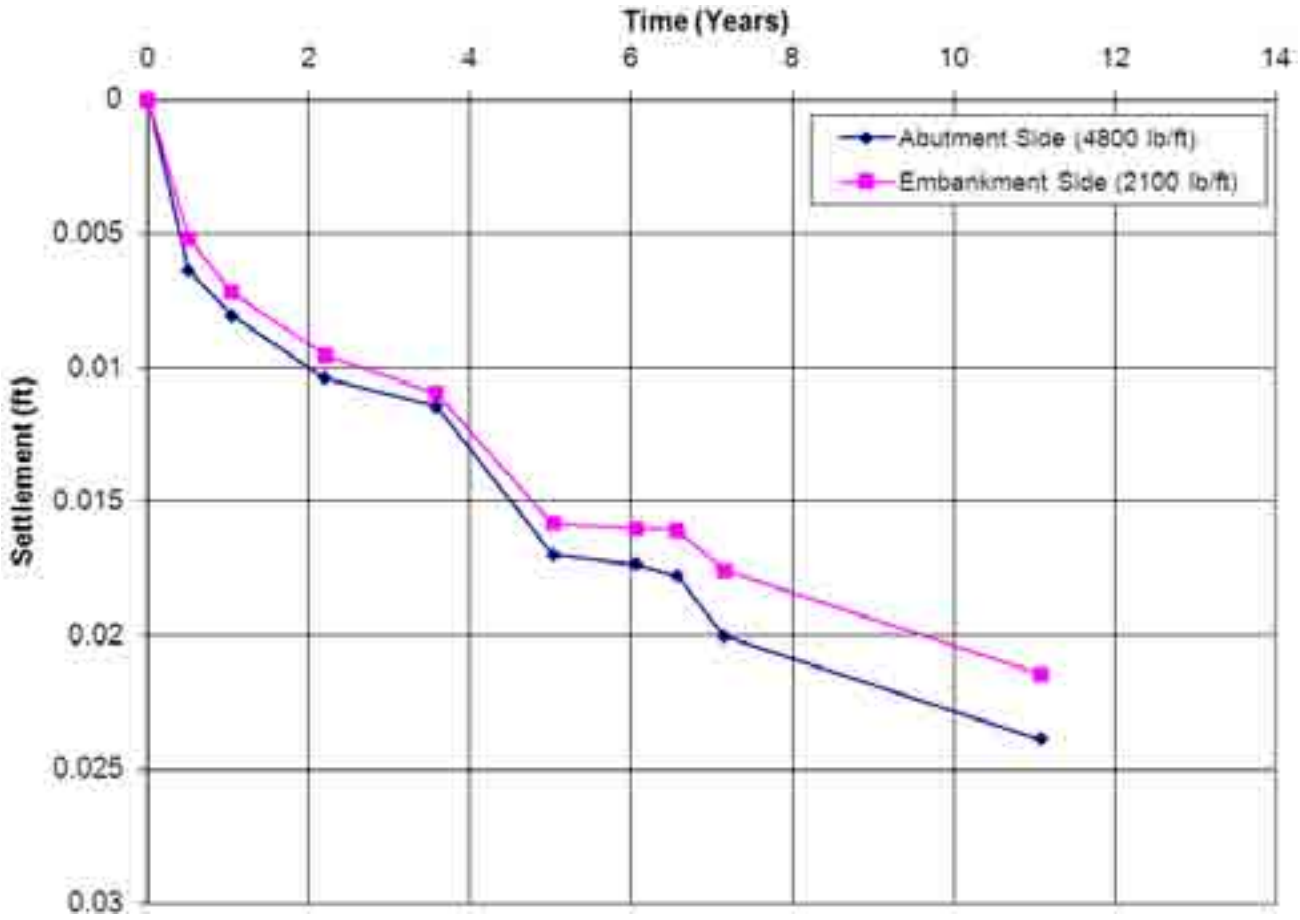

Figure 30. Graph. Settlement versus time for TFHRC tunnel.

Figure 31 is a log-time scale plot of figure 30 used to provide an estimate of vertical deformation within the GRS abutment at 100 years. The plot predicts the settlement at 100 years on the abutment side of the tunnel walls at 0.033 ft and on the embankment side at 0.030 ft.

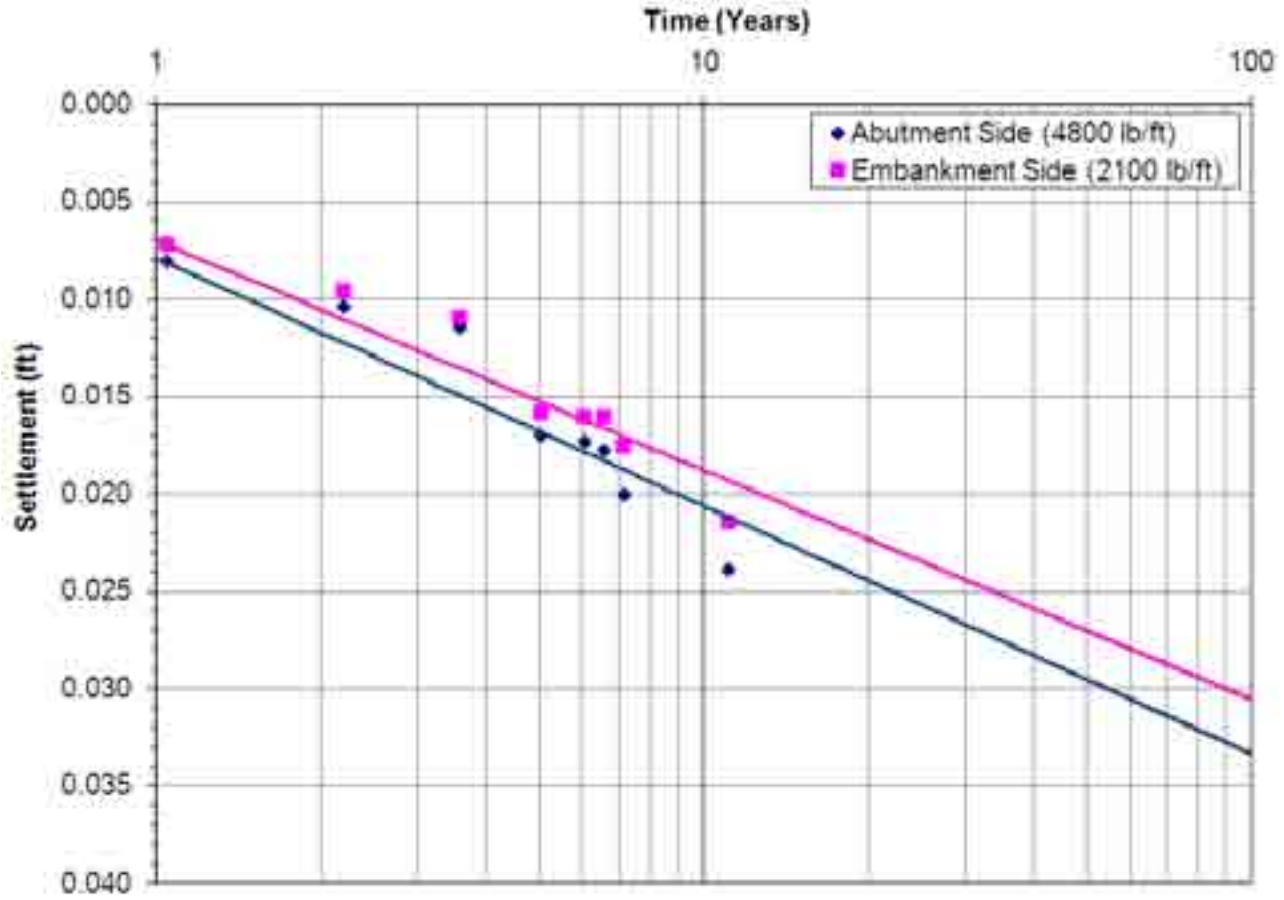

Figure 31. Graph. Settlement versus log-time to predict creep settlement for TFHRC tunnel at 100 years.

Several concrete box beam bridges were built by the Office of Federal Lands Highways and the U.S. Forest Service. The Lake Mamie and Twin Lake Bridges were built in Mammoth Lakes, CA, and have spans of 67 and 71 ft, respectively. Figure 32 and figure 33 are photos of these bridges. Figure 34 shows a cross sectional sketch of the GRS abutment behind the old stone abutment wall.[21] Only short-term settlement information is available for the bridges built in Mammoth Lakes, CA (see table 5).

Figure 32. Photo. GRS abutment behind historic stone abutment.

Figure 33. Photo. Concrete box bridge on GRS abutment in Mammoth Lake, CA.

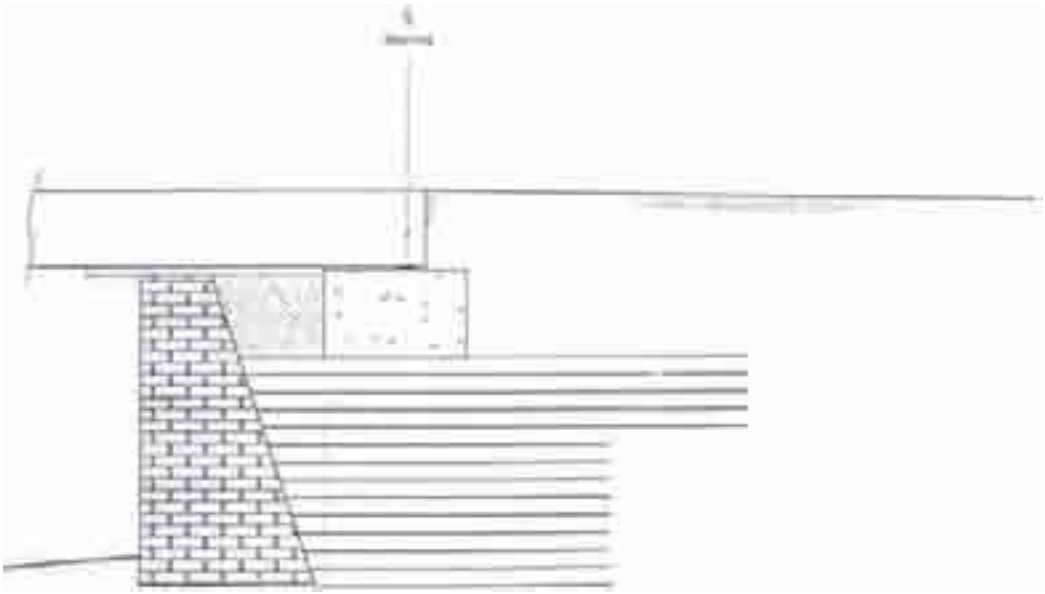

Figure 34. Illustration. Cross section of GRS abutment behind historic stone abutment.

Table 5. Summary of in-service GRS abutments.

Bridge	Date Built	Abutment	Average Total Settlement (ft)	Differential Settlement (ft)	Uniformity of Abutment Settlement (ΔS_{abut}/ width of bridge)	Angular Distortion (ΔS/ span length)
Lake Mamie	Fall 2000	Both	-0.013 at 3 days	No data	No data	No data
Twin Lake	Fall 2000	Both	-0.021 at 6 days	No data	No data	No data
Cecil Creek	June 2005	A	-0.098	0.013	0.0007	
		B	-0.02	0.002	0.0001	0.001
Big Lake	June 2005	A	0.007	0.040	0.002	
		B	-0.029	0.075	0.004	0.0005
Cut Off Creek	June 2005	A	0.078	0.050	0.003	
		B	0.072	0.001	0.00006	0.0001

Three bridges were also built in the Ouachita wildlife refuge in Louisiana (see figure 35 and figure 36). Each bridge has a span of 76 ft. The bridges are typically submerged under water for 6 months each year. Table 5 provides the settlement data for these bridges after 147 days of beam placement. The settlement performance of these bridges was well within acceptable criteria.

Figure 35. Photo. Concrete box bridge on GRS abutment in Ouachita wildlife refuge.

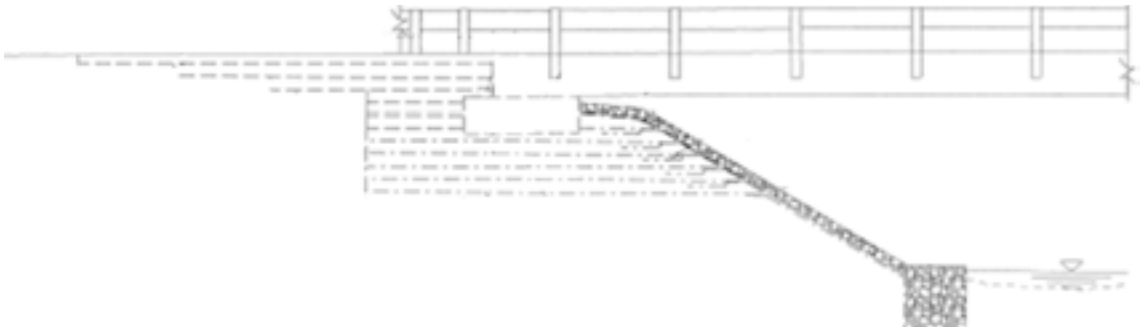

Figure 36. Illustration. Cross section of GRS abutments in Ouachita wildlife refuge.

4.2.2 Lateral Deformation

Lateral deformation has not been widely measured on in-service bridges because of difficulties in obtaining accurate long-term information. Previous GRS walls and abutments have performed well and have shown no reason for concern with lateral deformation. Theoretical calculations given in chapter 3 provide a method to determine the lateral deformation and strain based on an assumption of a zero loss of volume. The predicted average lateral deformation and lateral strain for the five previously discussed in-service bridges are shown in table 6.

Table 6. Predicted lateral deformations of five in-service bridges.

Bridge	Average Abutment Height H (ft)	Width of Bridge Bearing Area + Setback $b + a_b$ (ft)	Average GRS Mass Settlement D_v (ft)	Calculated Lateral Deformation $D_L = (2(b + a_b)*D_v)/H$ (ft)	Calculated Lateral Strain ε_L
Vine Street	11.36	2.64	0.023	0.011	0.004
Glenburg Road	13.01	2.14	0.083	0.027	0.013
Huber Road	16.73	2.64	0.015	0.005	0.002
Bowman Road	16.69	3.64	0.047	0.02	0.005
Tiffin River	19.26	5.14	0.089	0.047	0.009

Of the five in-service bridges shown in table 3, lateral deformation was only measured for Tiffin River Bridge. Measuring the horizontal movement was difficult due to the seasonal movement of the survey pole. The pole foundation extended approximately 4 ft below the ground surface. In dry periods, the data suggest that the pole settled and tipped. The pole then rebounded after soil moisture returned to normal levels. Attempts were made to correct the pole location by using back-site readings. However, due to the fact that many of the measured movements were smaller than the apparent movement of the survey pole over the long term, it is difficult to get a precise absolute movement. This is particularly true for the lateral deformation movement of abutment wall faces. By comparing the distance between both abutment faces, however, the effect of pole movement is minimized. While this does not allow the movement of each abutment to be evaluated independently, it does provide a measure of the average wall maximum bulge between the two abutment wall faces. Figure 37 shows a comparison between the calculated and measured lateral deformation as previously explained for Tiffin River Bridge (equation 11). The theoretical calculation matches very closely, within the ±0.005-ft error of the EDM system.

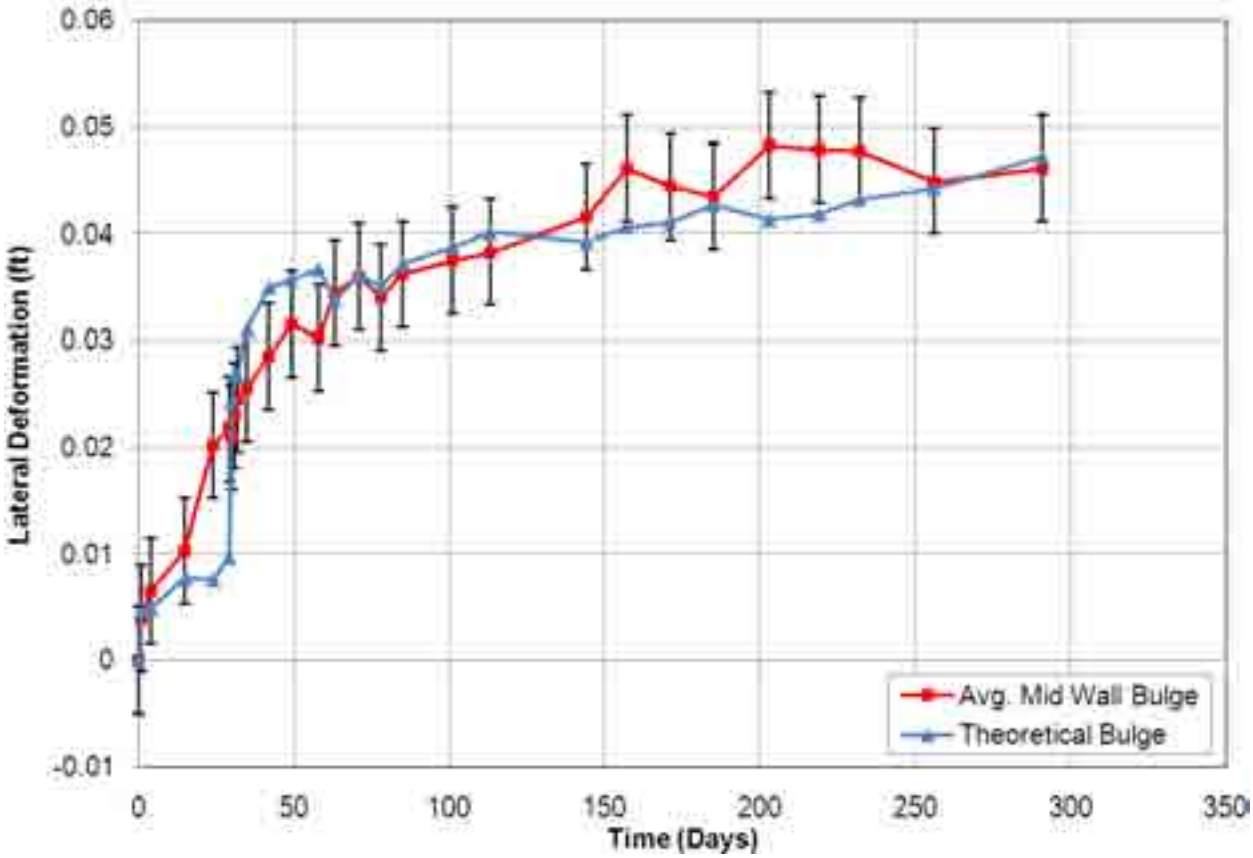

Figure 37. Graph. Measured and calculated lateral deformation on the Tiffin River Bridge GRS abutment.

4.3 THERMAL CYCLES

Thermal cycles occur on every bridge structure due to daily and seasonal temperature variations. The severity of the expansion and contraction depends on the coefficient of thermal expansion of the bridge. However, based on the experience of in-service GRS-IBS bridges with spans of up to 140 ft, the performance of GRS-IBS is not affected by thermal cycles. GRS-IBS accommodates movement related to thermal cycles, so the effect on the abutment is minimal.

GRS-IBS accommodates movement through the integrated transition behind the beam ends. The road base is wrapped with geosynthetic and is then well-compacted directly against the beam end. The wrapped face confines the soil and allows for the beam to contract without the fill behind the beam ends sloughing off to fill the void. As a result, excess pressures behind the beam during expansion are also avoided. The road base is not only wrapped vertically but also laterally to prevent lateral spread.

The performance of Tiffin River Bridge, the longest GRS-IBS steel bridge span (140 ft), has been monitored since construction.[(22)] Vibrating wire earth pressure cells were installed on the back wall of each abutment to measure lateral pressures between the superstructure and the integrated approach due to expansion and contraction of the steel girders (see figure 38 and figure 39). The average lateral earth pressure changes in magnitude with both daily and seasonal temperature effects (see figure 40). During the fall and winter (contraction), the lateral pressure decreased to

about 62 lb/ft^2. During the spring and summer (expansion), the lateral pressure increased to as high as about 700 lb/ft^2.[22] After one thermal cycle, it appears that the lateral pressure is nonlinear with temperature and displays hysteretic behavior. Monitoring continues, however, to determine the effect after multiple thermal cycles.

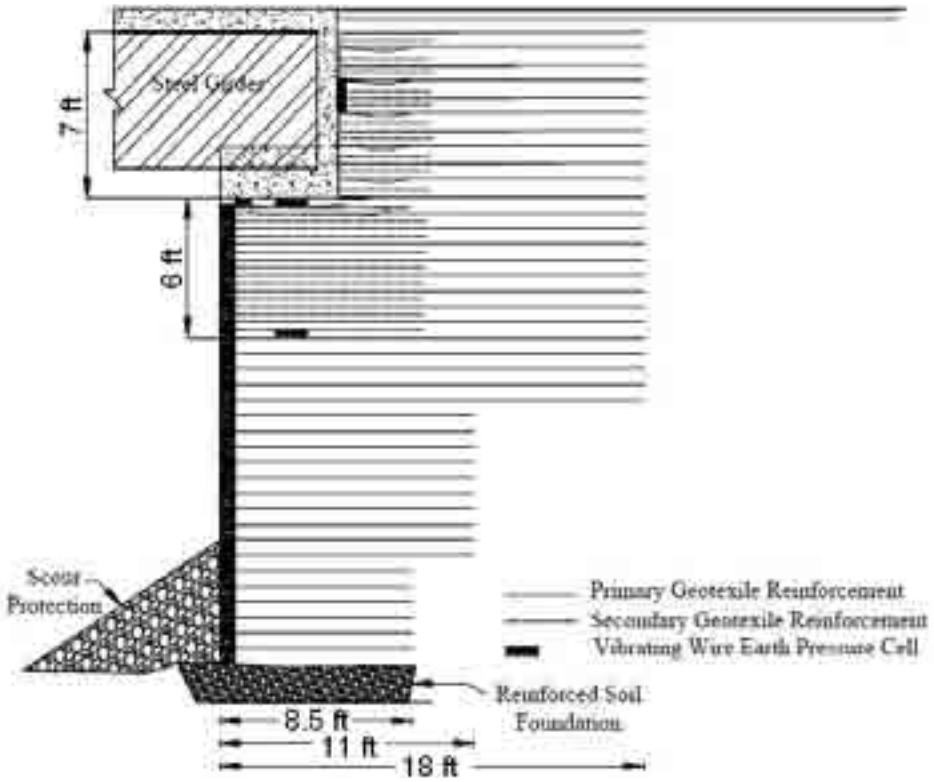

Figure 38. Illustration. Instrumentation for Tiffin River Bridge.

Figure 39. Photo. Pressure cells behind back wall on Tiffin River Bridge.

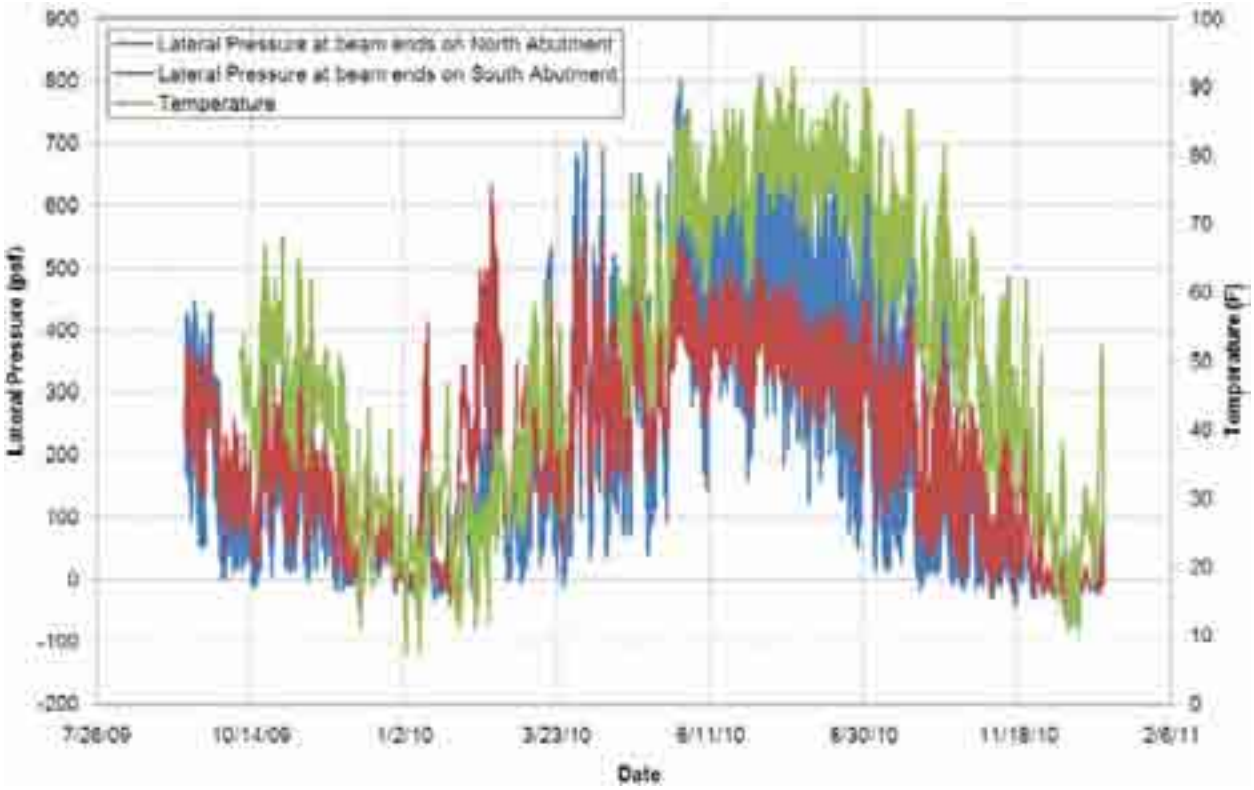

Figure 40. Graph. Average lateral pressure on back wall for Tiffin River Bridge.

APPENDIX A. PULL-OUT TEST RESULTS

As described in chapter 1, block pull-out and connection force is not an issue in GRS walls and abutments built with modular block facings because of the frequency of reinforcement between each layer of block. Many case studies have shown that a frictional connection between the modular blocks and the geotextile is compatible with deformations of the GRS composite mass. The facing blocks strain with the GRS mass, adjusting to lateral loads in order to maintain equilibrium with lateral thrust. In other words, if the GRS mass strains laterally 0.5 percent, then the facing will also displace that amount without attracting loads against the face.[9]

The compatibility of the frictional connection method has been illustrated through performance tests. After a vertical stress of 26 kips/ft^2, the performance test for Defiance County, OH, showed that the modular facing blocks remained frictionally connected to the GRS mass.[1] Similar results were seen in other tests. For example, a GRS pier built at TFHRC was loaded to 19 kips/ft^2 to show that the pier maintained its rectangular shape without the loss of any of the facing blocks (see figure 41). The frictional capacity between the blocks and the GRS mass was not exceeded even after extreme vertical loading conditions.

Figure 41. Photo. TFHRC pier test.

Nevertheless, it is important to understand the general capacity of the frictional connection method and the overall mechanics of the GRS system. For this reason, the following block pull-out test was devised to determine the amount of force required to mobilize a modular block out of the face of the wall (the pull-out force). The test was performed on blocks at different heights along the GRS wall to determine the relationship between the normal force on top of the block and the required pull-out force.

A.1 SETUP

To evaluate the frictional capacity, block pull-out tests were conducted on an actual GRS wall to quantify the amount of force necessary to move the block relative to the geotextile (see figure 42). The test was performed on segmental retaining wall (SRW) blocks frictionally connected to a 2,400 lb/ft geotextile. The setup for the test is shown in figure 43. The block pull-out tests were performed for nearly every course of blocks on a 12-ft-high wall, as outlined in the following procedure. Note that the same setup procedure can also be used on CMU blocks.

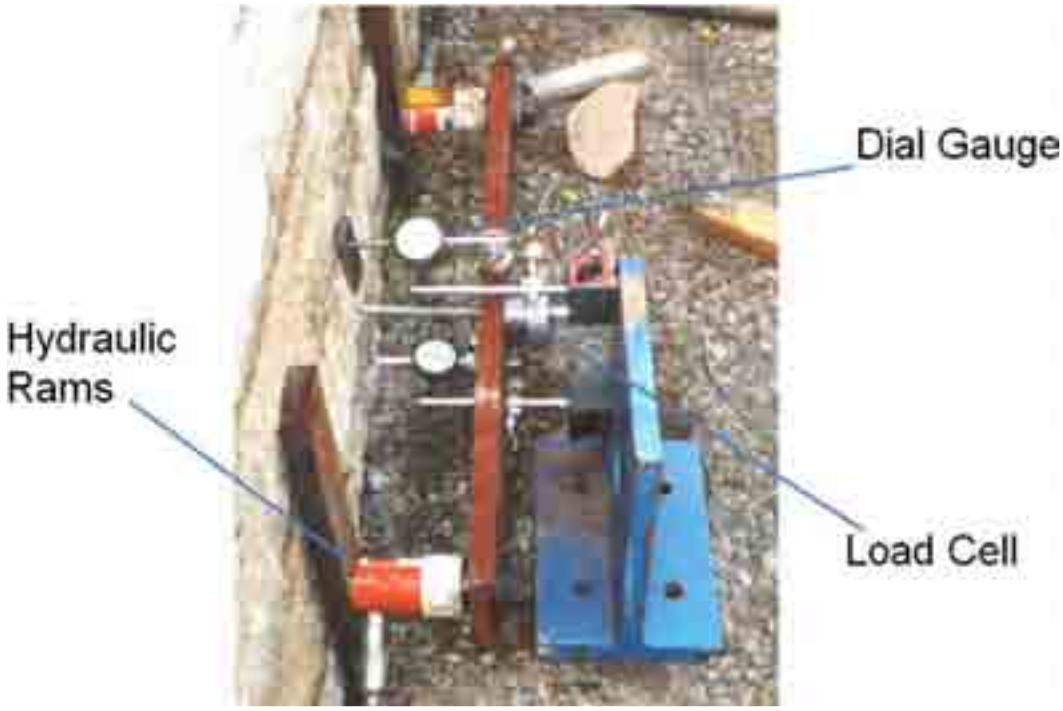

Figure 42. Photo. Block pull-out test on GRS wall.

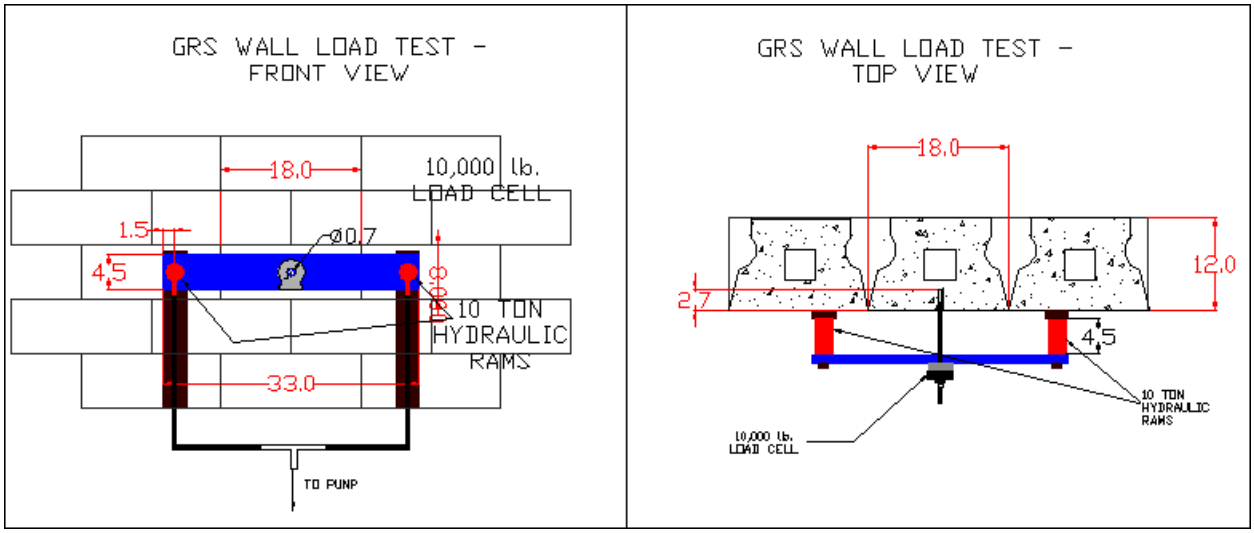

Figure 43. Illustration. Block pull-out test setup.

The test apparatus depicted in figure 42 and figure 43 includes the following:

- 10,000-lb load cell.
- Strain indicator box to measure the load (connects to load cell).
- Manual hydraulic pump with hoses for connecting the pump to the jacks.
- Two small 20-kip jacks.
- Two dial gauges for measuring displacement.
- Two magnetic bases for holding and positioning the dial gauges.
- 0.375-inch-diameter drop-in anchors.
- 0.375-inch-diameter threaded rod.
- Metal bar on which to connect the jacks.
- C-clamp.
- Metal bars.
- Hammer drill with 0.5-inch drill bit.

The apparatus is connected to the block according to the following steps:

1. Using a 0.5-inch drill bit, drill a hole in the center of the block to a suitable depth (approximately 2.67 inches).
2. Set the anchor using the setting tool.
3. Screw the threaded rod into the anchor in the block and make sure it is tight.
4. Make two flat spots on the top and bottom of the face of the block (above and below the rod).
5. Attach metal plates to the flat spots using epoxy.

A.2 PROCEDURE

Once the test apparatus is set up and properly connected to the block, the following procedure can be used to determine the block pull-out force:

1. Zero the two dial gauges.
2. Zero the load gauge.
3. Take initial readings for the top and bottom dial gauges at zero load.

4. Record the values of the initial readings.

5. Turn on the pump.

6. Add 50 lb to the jacks by manually pumping the arm of the pump.

7. Record displacement values at 0, 1, and 3 min for load values beginning at 50 lb and increasing in increments between 50 and 200 lb depending on the rate of the block displacement.

8. Stop the test when the block is displaced outward approximately 0.5 inches.

9. Take a final displacement reading at a load of zero.

A.3 TEST RESULT FOR SRW BLOCKS

Block pull-out capacity was measured at various heights along the GRS wall (2, 3, 4, 7, 8, 9, 10, 11, 12, 13, 15, 17, and 18 rows down). The load-displacement behavior for each test was recorded. In all cases, the block did not displace until the frictional capacity was exceeded. For example, the load displacement behavior is shown in figure 44 for a block that was seven rows down from the top with a normal force equal to 425 lb on top of it. The same trend is shown in figure 45 for a block that was 11 rows down from the top with a normal force equal to 765 lb on top of it, except the force required to move the block was higher. The same trend was true for the remaining tests.

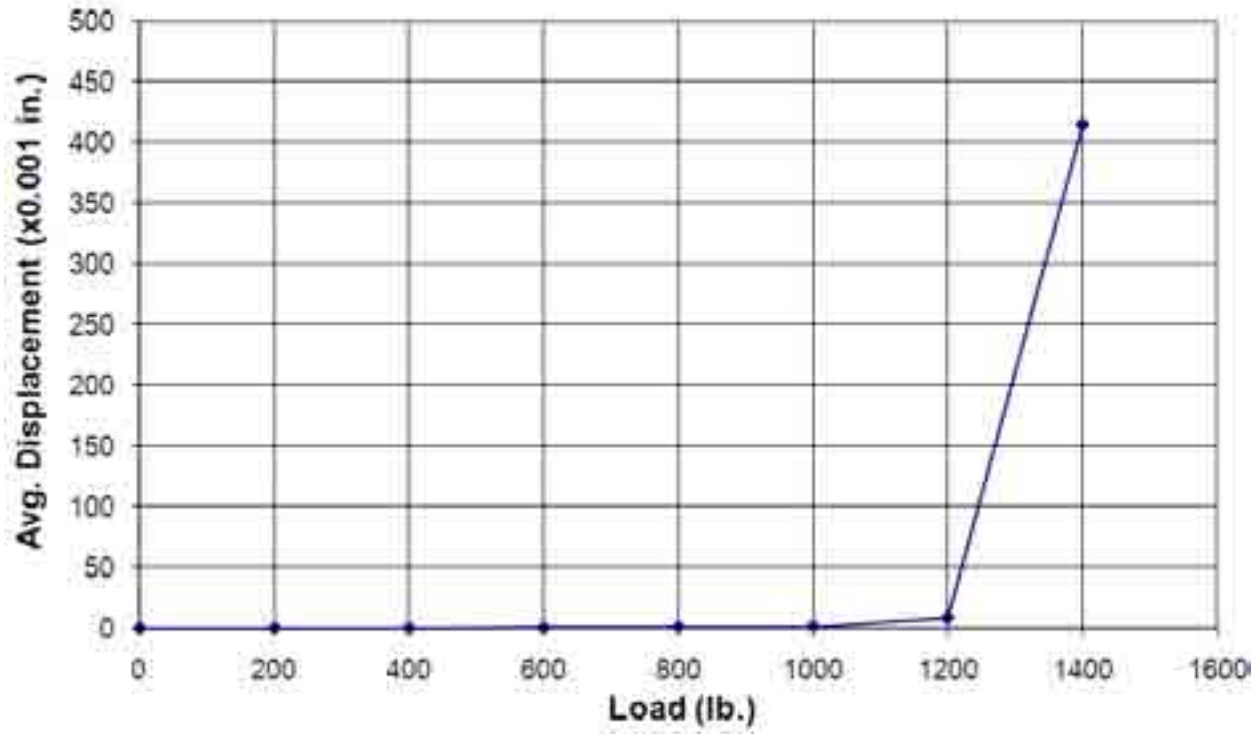

Figure 44. Graph. Pull-out test results for an SRW block seven rows from the top.

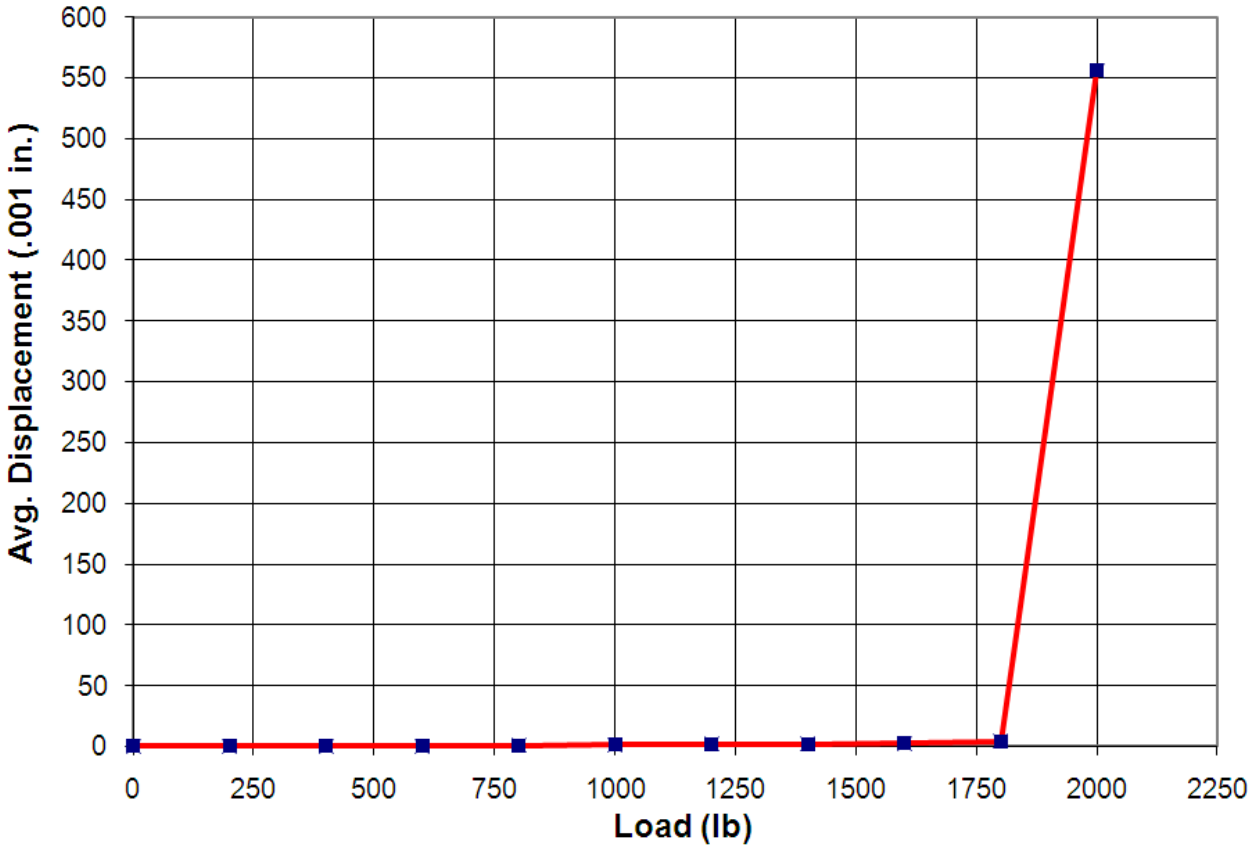

Figure 45. Graph. Pull-out test results for an SRW block 11 rows from the top.

The results show that a fairly linear relationship exists between the normal force on top of the block, which corresponds to the number of blocks down from the top of the wall, and the amount of force necessary to initiate block movement (see figure 46). The pull-out capacity for the experiment was chosen by reviewing the load versus displacement for the value directly before the greatest change in displacement.

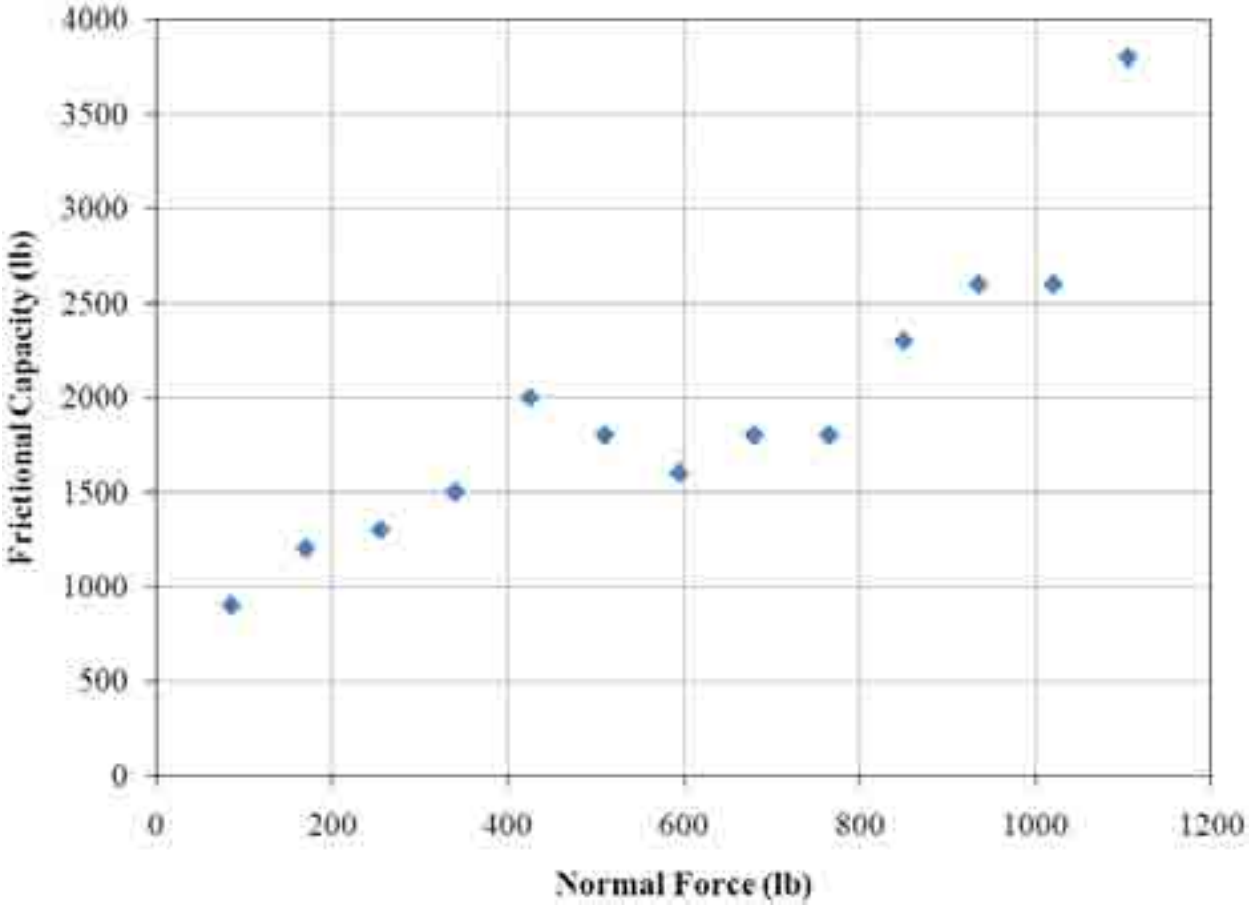

Figure 46. Graph. Pull-out test results in terms of normal force for SRW blocks.

The graph shows that the greater the normal force available due to the added weight of the blocks from above, the greater the block pull-out capacity. In a typical abutment, the thrust at the face is considerably lower (see chapter 1). Therefore, block pull-out and connection force is not a concern with GRS walls and abutments under normal conditions. It may, however, be a factor in designing for extreme events, seismic or impact. To add conservatism to the design and prevent any issues at the top of the wall (where the normal forces are the lowest), the top three courses of blocks are filled with a concrete fill mix and rebar to tie these blocks together.[(1)] It should be noted that although the pull-out tests were performed on SRW blocks, similar results would occur with CMU facing elements.

APPENDIX B. PREDICTION DATA FOR ANALYTICAL EQUATIONS

B.1 INTRODUCTION

Seventeen tests were used to validate the soil-geosynthetic capacity and required reinforcement strength equations. The complete set of data from these tests is presented in table 7.

Table 7. Prediction data for large-scale tests.

Test	Reference No.	σ_c (lb/ft^2)	S_v (inch)	T_f (lb/ft)	d_{max} (inch)	c (lb/ft^2)	f (degrees)	H (ft)	$q_{rupture}$ (lb/ft^2)	γ (lb/ft^3)
GSGC 1	10	710	None	–	1.3	1,462	50	6.5	–	153
GSGC 2	10	710	8	4,800	1.3	1,462	50	6.5	56,403	153
GSGC 3	10	710	16	9,600	1.3	1,462	50	6.5	36,558	153
GSGC 4	10	710	16	4,800	1.3	1,462	50	6.5	27,157	153
GSGC 5	10	0	8	4,800	1.3	1,462	50	6.5	39,691	153
Elton and Patawaran 1	23	0	6	620	0.5	576	40	5	4,805	121
Elton and Patawaran 2	23	0	12	620	0.5	576	40	5	2,695	121
Elton and Patawaran 3	23	0	6	960	0.5	576	40	5	6,392	121
Elton and Patawaran 4	23	0	6	1,025	0.5	576	40	5	6,100	121
Elton and Patawaran 5	23	0	6	1,300	0.5	576	40	5	8,398	121
Elton and Patawaran 6	23	0	6	1,400	0.5	576	40	5	8,293	121
Elton and Patawaran 7	23	0	6	1,700	0.5	576	40	5	9,589	121
NCHRP 1	7	0	8	1,400	1	418	37.3	15	7,312	117
NCHRP 2	7	0	8	4,800	1	418	37.3	15	17,757	117
Defiance 1	24	0	8[a]	2,400	0.5	0	48.7	6.4	11,320	110
Defiance 2	24	0	8[a]	4,800	0.5	0	48.7	6.4	21,412	110
Vegas Mini Pier	20	0	6[a]	2,400	1	576	40	8	20,890	121

[a] Two layers of a bearing bed reinforcement at 4 inches were placed at the top of the mass.
GSCG = Generic Soil-Geosynthetic Composite.
NCHRP = National Cooperative Highway Research Program.

B.2 SOIL-GEOSYNTHETIC CAPACITY EQUATION

The load-carrying capacity of a GRS wall and abutment ($q_{ult,an,c}$) can be evaluated using an analytical formula (equation 3). For this equation, the calculated capacity matches well with the measured capacity from large-scale tests (see figure 12). The numerical results of this comparison are presented in table 8. Note that for long-term design, cohesion (c) and confining stress (σ_c) are assumed to equal zero and should not be accounted for.

Table 8. Soil-geosynthetic capacity equation validation results.

Test	Reference No.	$q_{measured}$ (lb/ft^2)	q_{calc} (lb/ft^2)
GSGC 1	10	16,085	12,680
GSGC 2	10	56,403	51,181
GSGC 3	10	36,558	39,545
GSGC 4	10	27,157	26,113
GSGC 5	10	39,691	46,522
Elton and Patawaran 1	23	4,805	5,327
Elton and Patawaran 2	23	2,695	3,175
Elton and Patawaran 3	23	6,392	6,915
Elton and Patawaran 4	23	6,100	7,228
Elton and Patawaran 5	23	8,398	8,502
Elton and Patawaran 6	23	8,293	8,816
Elton and Patawaran 7	23	9,589	10,403
NCHRP 1	7	8,356	7,291
NCHRP 2	7	17,757	20,347
Defiance 1	24	13,370	11,322
Defiance 2	24	25,068	20,180
Vegas Mini Pier	20	20,890	18,258

GSCG = Generic Soil-Geosynthetic Composite.
NCHRP = National Cooperative Highway Research Program.

B.3 REQUIRED REINFORCEMENT STRENGTH EQUATION

For the required reinforcement strength equation (equation 13), the calculated strength matches well with the actual strength at rupture from large-scale tests (see figure 16). The biggest differences occur with some of the GSCS tests, which had a uniform confining pressure applied.[(10)] This confining stress will likely not be present in an actual GRS-IBS application. The numerical results of this comparison are presented in table 9. Note that for long-term design, the cohesion (c) and confining stress (σ_c) is assumed to equal zero and should not be accounted for.

Table 9. Required reinforcement strength equation validation results

Test	Reference No.	T_{actual} (lb/ft)	T_{calc} (lb/ft)
GSGC 2	10	4,800	5,483
GSGC 3	10	9,600	8,633
GSGC 4	10	4,800	5,274
GSGC 5	10	4,800	4,069
Elton and Patawaran 1	23	620	632
Elton and Patawaran 2	23	620	712
Elton and Patawaran 3	23	960	975
Elton and Patawaran 4	23	1,025	912
Elton and Patawaran 5	23	1,300	1,408
Elton and Patawaran 6	23	1,400	1,385
Elton and Patawaran 7	23	1,700	1,665
NCHRP 1	7	1,400	1,902
NCHRP 2	7	4,800	4,587
Defiance 1	24	2,400	2,857
Defiance 2	24	4,800	5,254
Vegas Mini Pier	20	2,400	2,944

GSCG = Generic Soil-Geosynthetic Composite.
NCHRP = National Cooperative Highway Research Program.

ACKNOWLEDGEMENTS

The interim implementation manual and synthesis report have been reviewed by technical experts in various disciplines: geotechnical, structural, hydraulic, maintenance, and pavement engineering. The authors recognize the efforts and contributions of many members of the FHWA for this work including Daniel Alzamora, Scott Anderson, Silas Nichols, Larry Arneson, Kornel Kerenyi, Joseph Krolak, Rich Barrows, Brian Collins, and Jorge Pagán.

The authors also recognize the contributions of other technical reviewers on this manual including Jim Collin, Erik Loehr, Paul Macklin, Christopher Meehan, Al Ruckman, Naresh Samtani, and Calvin VanBuskirk.

REFERENCES

1. Adams, M., Nicks, J., Stabile, T., Wu, J., Schlatter, W., and Hartmann, J. (2010). *Geosynthetic Reinforced Soil Integrated Bridge System—Interim Implementation Guide*, Report No. FHWA-HRT-11-026, Federal Highway Administration, McLean, VA.

2. Geo-Institute, Committee on Shallow Foundations. (1999). *Shallow Foundations on Reinforced Soil,* American Society of Civil Engineers, Reston, VA.

3. Berg, R., Christopher, B., and Samtani, N. (2009). *Design of Mechanically Stabilized Earth Walls and Reinforced Soil Slopes—Volume 1*, Report No. FHWA-NHI-10-024, National Highway Institute, Federal Highway Administration, Arlington VA.

4. Wu, J.T.H. (1994). *Design and Construction of Low Cost Retaining Walls: The Next Generation in Technology*, Report No. CTI-UCD-1-94, Colorado Transportation Institute, Denver, CO.

5. Adams, M.T., Ketchart, K., Ruckman, A., DiMillio, A., Wu, J.T.H., and Satyanarayana, R. (1999). "Reinforced Soil for Bridge Support Application on Low Volume Roads." Presented at the Seventh International Conference on Low-Volume Roads, *Transportation Research Record 1652*, pp. 150–160.

6. Koklanaris, M. (2000). "Geosynthetic Reinforced Soil Structures Can Carry the Load," *Public Roads*, Federal Highway Administration, Washington, DC.

7. Wu, J.T.H., Lee, K.Z.Z., Helwany, S.B., and Ketchart, K. (2006). *Design and Construction Guidelines for GRS Bridge Abutment with a Flexible Facing*, Report No. 556, National Cooperative Highway Research Program, Washington, DC.

8. Adams, M.T. (2010). "GRS Technology and the GRS Integrated Bridge System." Presented at Eugene Workshop, Local Technical Assistance Program, Eugene, OR.

9. Adams, M.T. (1997). "Performance of a Prestrained Geosynthetic Reinforced Soil Bridge Pier," *Mechanically Stabilized Backfill*, Wu, J.T.H (Ed.), pp. 35–53, Balkema, Rotterdam, Netherlands.

10. Wu, J.T.H., Pham, T.Q., and Adams, M.T. (2011). *Composite Behavior of Geosynthetic-Reinforced Soil (GRS) Mass*, Draft, Federal Highway Administration, McLean, VA.

11. Wu, J.T.H. (2001). *Revising the AASHTO Guidelines for Design and Construction of GRS Walls*, Report No. CDOT-DTD-R-2001-6, Colorado Department of Transportation, Denver, CO.

12. Wu, J.T.H., Lee, K.Z.Z., and Pham, T. (2006). "Allowable Bearing Pressure of Bridge Sills on GRS Abutments with Flexible Facing," *Journal of Geotechnical and Geoenvironmental Engineering 132*(7), pp. 836–841, American Society of Civil Engineers.

13. Adams, M.T. (2008). "The Bridge of Defiance County," *Geosynthetics, 26*(2), pp 14–16, 18, 20–21, Industrial Fabrics Association International, Roseville, MN.

14. Wu, J.T.H. and Adams, M.T. (2007). "Myth and Fact on Long-Term Creep of GRS Structures," *Geotechnical Special Publication No. 165*, Geosynthetics in Reinforcement and Hydraulic Applications, Proceedings, Geo-Denver 2007, American Society of Civil Engineers, Denver, CO.

15. Ketchart, K. and Wu, J.T.H. (1996). *Long-Term Performance Tests of Soil-Geosynthetic Composites*, Report No. CDOT-CTI-96-1, Colorado Department of Transportation, Denver, CO.

16. Wu, J.T.J., Ketchart, K., and Adams, M. (2001). *GRS Bridge Piers and Abutments*, Report No. FHWA-RD-00-038, Federal Highway Administration, McLean, VA.

17. Morrison, K.F., Harrison, F.E., Collin, J.G., Dodds, A., and Amdt, B. (2006). *Shored Mechanically Stabilized Earth (SMSE) Wall Systems Design Guidelines*, Report No. FHWA-CFL/TD-06-001, Federal Highway Administration, Central Federal Lands Highway Division, Lakewood, CO.

18. Bell, A.L. (1915). "The Lateral Pressure and Resistance of Clay and Supporting Power of Clay Foundations," *Min. Proceeding of Institute of Civil Engineers 199*, pp. 233–272.

19. Samtani, N.C. and Nowatzki, E.A. (2006). *Soils and Foundations Reference Manual*, Report No. FHWA-NHI-06-088, National Highway Institute, Federal Highway Administration, Arlington, VA.

20. Adams, M.T., Lillis, C.P., Wu, J.T.H., and Ketchart, K. (2002). "Vegas Mini Pier Experiment and Postulate of Zero Volume Change." Proceedings, Seventh International Conference on Geosynthetics, pp. 389–394, Nice, France.

21. Keller, G.R. and Devin, S. (2003). "Geosynthetic Reinforced Soil Bridge Abutments," *Transportation Research Board 1819*(2), pp. 362–368, Eighth International Conference on Low Volume Roads, Reno, NV.

22. Warren, K.A., Schlatter, W., Adams, M., Stabile, T., and LeGrand, D. (2011). "Thermal Effects and Deformations Associated with a Large, Single Span Bridge Supported by a GRS Integrated Bridge System." Proceedings, GeoFrontiers 2011, Dallas, TX.

23. Elton, D.J. and Patawaran, M.A.B. (2005). *Mechanically Stabilized Earth (MSE) Reinforcement Tensile Strength from Tests of Geotextile Reinforced Soil*, Alabama Highway Research Center, Auburn University, Auburn, AL.

24. Adams, M.T., Schlatter, W., and Stabile, T. (2007). "Geosynthetic-Reinforced Soil Integrated Abutments at the Bowman Road Bridge in Defiance County, Ohio." Proceedings, Geo-Denver 2007, American Society of Civil Engineers, Denver, CO.

HRDI-40/01-11(300)E